Atmos. Chem. Phys. Discuss., doi:10.5194/acp-2016-270, 2016
Manuscript under review for journal Atmos. Chem. Phys.
Published: 25 April 2016

Atmospheric Chemistry and Physics Discussions

Long-term assessment of airborne radiocesium after the Fukushima nuclear accident: Re-suspension from bare soil and forest ecosystems

M. Kajino[1, 2], M. Ishizuka[3], Y. Igarashi[1], K. Kita[4], C. Yoshikawa[5], and M. Inatsu[6]

[1]{Meteorological Research Institute (MRI), Japan Meteorological Agency (JMA), Tsukuba, Ibaraki, Japan}

[2]{RIKEN Advanced Institute for Computational Science (AICS), Kobe, Hyogo, Japan}

[3]{Kagawa University, Takamatsu, Kagawa, Japan}

[4]{Ibaraki University, Mito, Ibaraki, Japan}

[5]{Japan Agency for Marine-Earth Science and Technology (JAMSTEC), Yokosuka, Kanagawa, Japan}

[6]{Hokkaido University, Sapporo, Hokkaido, Japan}

Correspondence to: M. Kajino (kajino@mri-jma.go.jp)

Abstract

The long-term effect of ^{137}Cs re-suspension from contaminated soil and forests due to the Fukushima nuclear accident has been quantitatively assessed by numerical simulation, a field experiment on dust emission flux in the contaminated area (Namie, Fukushima), and air concentration measurements inside (Namie) and outside (Tsukuba, Ibaraki) the contaminated area. The assessment period is for the year 2013 just after the start of the field experiments, December 14, 2012. The ^{137}Cs concentrations at Namie and Tsukuba were approximately 10^{-1} – 1 and 10^{-2} – 10^{-1} mBq/m^3, respectively. The observed monthly median concentration at Namie was one to two orders of magnitude larger than that at Tsukuba. This observed difference between the two sites was consistent with the simulated difference, indicating successful modeling of ^{137}Cs re-suspension and atmospheric transport. The estimated re-suspension rate was approximately 10^{-6} /d, which was significantly lower than the decreasing

Atmos. Chem. Phys. Discuss., doi:10.5194/acp-2016-270, 2016
Manuscript under review for journal Atmos. Chem. Phys.
Published: 25 April 2016

Atmospheric Chemistry and Physics Discussions

rate of the ambient gamma dose rate in Fukushima prefecture (10^{-4} – 10^{-3} /d) as a result of radioactive decay, land surface processes (migration in the soil and biota), and decontamination. Consequently, re-suspension contributed negligibly to reducing ground radioactivity. The dust emission model could account for the air concentration of ^{137}Cs in winter, whereas the summer air concentration was underestimated by one to two orders of magnitude. Re-suspension from forests at a constant rate of 10^{-7} /h, multiplied by the green area fraction, quantitatively accounted for the air concentration of ^{137}Cs at Namie and its seasonal variation. The simulated contribution of dust re-suspension to the air concentration was 0.6 – 0.8 in the cold season and 0.1 – 0.4 in the warm season at both sites; the remainder of the contribution was re-suspension from forest. The re-suspension mechanisms, especially through the forest ecosystems, remain unknown, and thus the current study is the first but crude estimation of the long-term assessment of radiocesium re-suspension. Further study will be needed to understand the re-suspension mechanisms and to accurately assess the re-suspension mechanisms through field experiments and numerical simulations.

Keywords: Atmospheric radioactivity, Re-suspension, Dust emission, Unknown re-suspension source, Aerosol, Numerical simulation, Budget analysis

1 Introduction

The Fukushima Daiichi Nuclear Power Plant (FDNPP) accidentally released nuclear fission products into the atmosphere and ocean environment following the catastrophic earthquake and tsunami in March 2011. The accident caused serious contamination of the ground soil over the Tohoku region (northeastern part of Japan, including Fukushima and Miyagi prefectures) and the Kanto region (eastern part of Japan, including Ibaraki, Tochigi, Gunma, and Chiba prefectures) (NRA, 2012). Since then, a number of studies have been conducted, particularly in the crisis phase of the disaster. These assessments include primary emission estimations (Chino et al., 2011; Danielache et al., 2012; Stohl et al., 2012; Terada et al., 2012; Katata et al., 2012a, 2012b; Winiarek et al., 2012, 2014; Hirao et al., 2013; Saunier et al., 2013; Katata et al., 2015; Yumimoto et al., 2016; Danielache et al., 2016), field observations (Masson et al., 2011, 2013; NRA, 2012; Kaneyasu et al., 2012; Adachi et al., 2013; Tsuruta et al., 2014; Hososhima and Kaneyasu, 2015; Igarashi et al., 2015; Oura et al., 2015), and numerical simulations (deterministic simulation: Chino et al., 2011; Morino et al., 2011; Yasunari et al., 2011; Stohl et al., 2012; Terada et al., 2012; Katata et al., 2012a, 2012b;

Atmos. Chem. Phys. Discuss., doi:10.5194/acp-2016-270, 2016
Manuscript under review for journal Atmos. Chem. Phys.
Published: 25 April 2016

Atmospheric Chemistry and Physics Discussions

Winiarek et al., 2012, 2014; Hirao et al., 2013; Saunier et al., 2013; Katata et al., 2015; Yumimoto et al., 2016; Danielache et al., 2016, deterministic simulation with sensitivity runs: Morino et al., 2013; Adachi et al., 2013; Groëll et al., 2014; Saito et al., 2015; Sekiyama et al., 2015; Quérel et al., 2016, uncertainty modeling and probabilistic forecast: Girard et al., 2016; Sekiyama et al., 2016, and multi-model inter-comparison and multi-model ensemble analysis: SCJ, 2014; Draxler et al., 2015) The targeted radionuclides were species with both short and long half-lives: ^{99}Mo-^{99m}Tc (half-life 65.9 – 6 h), ^{129m}Te (33.6 d), ^{131}I (8.02 d), ^{132}Te-^{132}I (3.2 d – 2.3 h), ^{134}Cs (2.07 y), ^{136}Cs (13.2 d), ^{137}Cs (30.1 y), ^{133}Xe (5.2 d), and ^{35}S (87.5 d).

In contrast, there have been few studies on the long-term (more than one year) quantitative assessment of radioactivity in the atmosphere associated with the Fukushima accident (Igarashi et al., 2015; Ishizuka et al., 2016; Kinase et al., 2016). More than 100,000 people were evacuated (METI, 2012), but most have still not been able to return to their homes and the public remains anxious about the safety of the affected areas. Radionuclides with long half-lives such as ^{134}Cs (2.07 y) and ^{137}Cs (30.1 y) are of particular concern. Following the Chernobyl accident there were several studies on the re-suspension and long-term assessment of these radionuclides, such as Holländer and Garger (1996), Garger et al. (1998), Hatano and Hatano (2003) and Garger et al. (2012). For example, Garger et al. (2012) estimated the re-suspension "descending trend" as having a half-life of 300 d based on the surface activity concentration of ^{137}Cs. In the case of the Fukushima accident, Igarashi et al. (2015) estimated the half-reduction time by fitting multi-component exponential functions based on the ^{137}Cs concentration at the Meteorological Research Institute, Tsukuba, as 5.9 d, 16 d, and 1.1 y. These estimates were based on the trend in the observed surface air concentrations of ^{137}Cs, and thus the contributions from advection, diffusion, emission and deposition terms were quantified.

There are thousands of monitoring posts situated in the contaminated area in Fukushima prefecture to measure the ambient gamma dose rate, but the data cannot be used for evaluating internal exposure: evaluation of internal exposure requires direct measurement of the surface air activity concentration. There are only a few observation sites that continuously measure the concentration of radiocesium (e.g., Igarashi et al., 2015; Ishizuka et al., 2016; Kinase et al., 2016). To assess the spatial distribution of the internal exposure hazard, 3D numerical simulation is necessary to interpolate values at locations where there are no measurements. The numerical simulation requires emission flux as a boundary condition.

Atmos. Chem. Phys. Discuss., doi:10.5194/acp-2016-270, 2016
Manuscript under review for journal Atmos. Chem. Phys.
Published: 25 April 2016

Atmospheric Chemistry and Physics Discussions

However, the mechanism and thus the radioactivity flux associated with the re-suspension of ^{137}Cs were unknown, despite extensive efforts based on field observations (e.g., Igarashi et al., 2015; Ishizuka et al., 2016; Kinase et al., 2016).

Garger et al. (2012) summarized the re-suspension sources following the Chernobyl accident as (1) dust emission, (2) human activity in fields, and on roads and construction sites, (3) forest fires, and (4) emissions from opening of the Chernobyl sarcophagus. Re-suspension sources (1) and (4) were considered in the present study. With respect to source (2), since Namie, Fukushima, is located in the evacuation zone, human activity has been extremely limited except for decontamination-related work. As to source (3), there is a low chance of forest fires in Japan given the high humidity but some open biomass burning is a possibility. Kinase et al. (2016) found no increase in ^{137}Cs concentration when the concentration of levoglucosan, a marker of biomass burning, was increased, and thus re-suspension due to biomass burning was not considered in the present study. In addition to the four sources of ^{137}Cs from the Chernobyl accident, re-suspension from terrestrial biota was considered as suggested by Kinase et al. (2016). They found substantial amounts of bioaerosols upon scanning electron microscopy examination of samples collected in the summer, when ^{137}Cs concentration was high.

In the present study, the long-term effect of radiocesium re-suspension from contaminated soil and terrestrial biota was quantitatively assessed using 3D numerical simulation, a field experiment on dust emission flux in a contaminated area (Namie, Fukushima), and air concentration measurements taken inside (Namie) and outside (Tsukuba, Ibaraki) the contaminated area. The current study is the first but crude estimation of the spatial budget of radiocesium via re-suspension since the re-suspension mechanisms, especially through forest ecosystems, remain unknown. By utilizing observational data collected both inside and outside of the contaminated area, together with 3D numerical simulation, we aimed to provide as robust a budget analysis as possible of the re-suspension, transport, and re-deposition of ^{137}Cs over the Tohoku and Kanto regions of Japan.

2 Numerical simulation

A brief description of the numerical method, such as processes considered in the model and simulation settings, are presented in this section, and detailed model formulations are

Atmos. Chem. Phys. Discuss., doi:10.5194/acp-2016-270, 2016
Manuscript under review for journal Atmos. Chem. Phys.
Published: 25 April 2016

described in Appendix A. Because the schemes and assumptions regarding the emissions are key to the current study, they are described in detail in the following subsections.

2.1 Lagrangian Model and simulation settings

Figure 1 shows the domain of the Lagrangian Model (LM) with model terrestrial elevations, covering 138 – 143 °E and 34 – 39 °N. The model domain covers the southern part of the Tohoku region (the northern mountainous part of the domain, including Yamagata, Miyagi, and Fukushima prefectures), and includes the FDNPP and highly polluted areas such as the Habitation-Restricted Zone (HRZ) (20 – 50 mSv/y) and Difficult-to-Return Zone (DRZ) (> 50 mSv/y) (METI, 2012). It also covers the Kanto region (or Kanto Plain, the largest plain in Japan, approximately 120 km × 120 km), a highly populated region that includes moderately polluted areas such as Tokyo, Gunma, Tochigi, Ibaraki, Saitama, and Chiba prefectures.

LM considers horizontal and vertical diffusion and advection, gravitational settling, dry and wet depositions, and radioactive decay. It uses simple parameterizations for dry and wet deposition schemes, and it can be driven by meteorological analysis data sets so that it does not require a meteorological model to predict detailed meteorological fields and variables. The model was designed to be easily handled and computationally efficient so that non-specialists of numerical simulations can conduct long-term assessments of atmospheric diffusion problems using their desktop or laptop computers. The LM was designed for rough budget estimates, as presented in the current study, or for sensitivity analyses using a number of parameters (e.g., Groëll et al., 2014; Girard et al., 2016; Quérel et al., 2016), rather than for process-oriented analysis (e.g., Morino et al., 2013; Katata et al., 2015) or sensitivity analyses of the physical and chemical parameters of aerosols (Adachi et al., 2013). Details of each process and parameter are described in Appendix A. Statistical error of a Lagrangian simulation is inversely proportional to the square of the number of Lagrangian particles (LPs). The statistical accuracy of the current simulation setting is discussed in Appendix B.

The Grid Point Value Meso-Scale Model (GPV-MSM) of the Japan Meteorological Agency (JMA) was used for meteorological analysis to calculate the transport of LPs. It covers 120 – 150 °E and 23 – 47 °N and provides 3 hourly and 16 pressure levels of 3D meteorological variables, from 1000 hPa to 100 hPa, with a horizontal grid resolution of approximately 11 km (Δlongitude = 0.125° and Δlatitude = 0.1°) and surface variables at twice the resolution as that for the 3D variables (Δlongitude = 0.0625° and Δlatitude = 0.05°). In the simulation, the

Atmos. Chem. Phys. Discuss., doi:10.5194/acp-2016-270, 2016
Manuscript under review for journal Atmos. Chem. Phys.
Published: 25 April 2016

Atmospheric Chemistry and Physics Discussions

whole model domain where LPs can travel is 138 – 143 °E, 34 – 39 °N and from ground surface to 500 hPa. For output of the model results, LP fields are converted to Eulerian concentration (Bq/m^3) and deposition (Bq/m^2) fields in the same horizontal space as the 3D variables but are vertically allocated from the ground surface to an altitude of 1 km at 100 m intervals. The observed surface air concentration was compared with the simulated mean concentration at 0 – 100 m above ground level (AGL).

2.2 Re-suspension from bare soil

Ishizuka et al. (2016) developed a re-suspension scheme for radiocesium from bare soil based on measurements on the ground at Namie High School, Tsushima Campus (denoted as Namie (Tsushima) in Table 1 and Fig. 1) in the DRZ.

$$F_{soil} = p_{20\,\mu m} F_M (1 - f_{forest}) B_{5\,mm}(t), \quad (1)$$

where F_{soil} is the ^{137}Cs dust re-suspension flux from soil (Bq/m^2/s), $p_{20\mu m}$ is the mass fraction of dust smaller than 20 μm in diameter against soil containing a maximum size of 2 mm particles, and varies depending on soil texture (2×10^{-9} for sand, 0.03 for loamy sand, 0.09 for sandy loam, and 0.32 for silt loam), F_M is the total dust mass flux (kg/m^2/s), f_{forest} is the forest area fraction, and $B_{5mm}(t)$ is the specific radioactivity of surface soil (from the surface to a depth of 5 mm) (Bq/kg) as a function of time since March 2011. The formula is based on the assumption that dust particles smaller than 20 μm in diameter originated from the surface soil and to a depth of 5 mm were suspended and transported through the atmosphere. F_M is formulated as being proportional to the cube of the friction velocity u_* (m/s) as described by Loosmore and Hunt (2002) and was applied to the dust emission:

$$F_M = 3.6\times10^{-9} u_*^3. \quad (2)$$

Since u_* is not available in GPV-MSM, u_* was estimated using a wind speed at 10 m AGL by assuming neutral stratification conditions.

$B_{5mm}(t)$ was derived from the combination of B_{obs}, the observed horizontal distribution of ^{137}Cs deposition obtained from an airborne radiological survey (NRA, 2012) (Bq/m^2) and r_{5mm}, the surface soil activity ratio of 0 – 5 mm to 0 – 5 cm obtained from a vertical profile measurement of ^{137}Cs in the ground soil at Namie High School (= 0.57 Bq/Bq) as

Atmos. Chem. Phys. Discuss., doi:10.5194/acp-2016-270, 2016
Manuscript under review for journal Atmos. Chem. Phys.
Published: 25 April 2016

Atmospheric Chemistry and Physics Discussions

$$B_{5\,\mathrm{mm}}(t) = \frac{B_{obs} r_{5mm} R_{decay}(t)}{5\times10^{-3}\,\rho_{b,soil}}, \quad (3)$$

where $\rho_{b,soil}$ is the bulk density of soil particles per unit volume in the ground space (kg/m^3) obtained from the porosity (0.4 m^3/m^3) and the density of dust particles (2650 kg/m^3). For R_{decay}, which is the decreasing rate of activity in the ground, only radioactive decay was considered for the re-suspension calculation. The decreasing rate due to other processes such as land surface processes (or migration in the soil and biota) and decontamination were not considered here. Also, suppression of dust emission due to soil moisture and snow cover was not considered. Therefore, it should be noted here that F_{soil} in Eq. (1) is considered as a maximum estimate of ^{137}Cs re-suspension flux from surface soil. Effects such as land surface processes, decontamination, and dust emission suppression due to snow cover are extensively discussed in Appendix C using ambient gamma dose rate measurements obtained by the monitoring posts (Table 1, Fig. 1b, and Fig. C1).

Eq. (1) is a function of soil texture. The areal fraction of soil texture of the model grid was obtained from the database of the advanced research Weather Research and Forecasting model version 3 (WRFV3; Skamarock et al., 2008). Sixteen categories of soil texture (Miller and White, 1998) with a 30 arcseconds resolution dataset can be obtained from the web after subscription at (http://www2.mmm.ucar.edu/wrf/users/download/get_sources_wps_geog.html, last access: 12 February 2016) and were re-categorized into the above-mentioned four categories and interpolated to the LM resolution (~11 km) as shown in Fig. 2a-c. Note that the loamy sand fraction is not presented because it is zero for the entire domain. The parameter f_{forest} (Fig. 2d) was also obtained from the database of WRFV3 and was calculated based on the 24 United States Geological Survey (USGS) Land Use Categories, which are constant over time. The Land Use Category dataset can also be obtained from the above website.

Ishizuka et al. (2016) validated their dust emission module by using a 1D model and observed the surface air concentration of ^{137}Cs at Namie in the winter. After applying the module to our 3D simulation, we found that the air concentration at Namie was underestimated by about one order of magnitude for the same period. The module was formulated based on physical parameters (such as u_*) but contains parameters obtained at a single location (such as r_{5mm} and $\rho_{b,soil}$) and under a fixed atmospheric condition (Ishizuka et al., 2016), whereas ideally parameters in Eqs. (1) – (3) should have considered variations among locations and atmospheric conditions for the 3D simulation. We set the parameter to 10 after adjusting the

Atmos. Chem. Phys. Discuss., doi:10.5194/acp-2016-270, 2016
Manuscript under review for journal Atmos. Chem. Phys.
Published: 25 April 2016

Atmospheric Chemistry and Physics Discussions

simulation results against the observed concentration of ^{137}Cs at Namie in the winter. This is one of the simplest top-down approaches for adjusting the emission flux according to the air concentration. The module requires improvement in the future as more reliable parameters become available for various conditions and locations.

2.3 Re-suspension from the forest ecosystems

The re-suspension mechanism of radiocesium from land ecosystems remains unknown. Kinase et al. (2016) found substantial amounts of bioaerosols (rather than mineral dust particles) in samples collected for scanning electron microscopy in the summer, when the ^{137}Cs concentration was high. This does not prove that the bioaerosol was carrying radiocesium, but that it could be a potential carrier. The behavior of Cs in the environment can be inferred by analogy with K, a congener of Cs. Potassium is a necessary and abundant element in plants and circulates between land ecosystems. The addition of potassium fertilizer to a rice field in Fukushima significantly reduced the Cs content of the rice (Ohmori et al., 2014). Substantial amounts of K-salt-rich particles, possibly emitted by active biota such as plants and fungi, and coated with secondary organic aerosols, were observed in pristine Amazonian rainforest (Pöhlker et al., 2012). The major areal fraction of the contaminated area in Fukushima is covered by biota-rich mountain forests (Figs. 1a, 2d, and 4a). Despite the differences in plant species and locations, it is plausible that water-soluble radiocesium circulating in the biota and soil in the forests was somehow re-emitted into the atmosphere and contributed to the surface air concentration. The re-suspension from the forest ecosystem was simply formulated as follows:

$$F_{forest} = f_{forest}\, f_{green}\, r_{const}\, B_{obs}\, R_{decay}(t), \quad (4)$$

where F_{forest} is the ^{137}Cs re-suspension flux from forest (Bq/m^2/s), f_{green} and r_{const} are the monthly green area fraction and the constant re-suspension coefficient (/s), respectively, and r_{const} is a tunable parameter to adjust the simulated air concentration of ^{137}Cs to that observed. In the current study, r_{const} is set to 10^{-7} /h by adjusting the simulation data using the observed ^{137}Cs concentration at Namie in the summer, when the re-suspension from soil was negligible due to the higher soil moisture content (following considerable rain) and lower wind speed. As with re-suspension from soil, only radioactive decay was considered for R_{decay} and the other processes were not considered. Unlike re-suspension from soil, precipitation might not suppress re-suspension from the forest ecosystems since substantial amounts of K-containing

Atmos. Chem. Phys. Discuss., doi:10.5194/acp-2016-270, 2016
Manuscript under review for journal Atmos. Chem. Phys.
Published: 25 April 2016

Atmospheric Chemistry and Physics Discussions

particles were observed in the wet season in the Amazon (Pöhlker et al., 2012 and references therein). The parameter f_{green} was obtained from the database of WRFV3 and was originally derived from satellite Advanced Very High Resolution Radiometer (AVHRR)/Normalized Difference Vegetation Index (NDVI) data (Gutman and Ignatov, 1998). Whereas f_{forest} remains constant, the monthly averaged f_{green} was used in order to reflect seasonal changes in the activity of the biota.

2.4 Emission from FDNPP (primary emission, additional emissions from the reactor buildings, and unexpected re-suspension associated with debris removal operations)

Katata et al. (2015), the Japan Atomic Energy Agency (JAEA)'s latest estimate of the primary emission from FDNPP, was applied for the emergency situation of March 2011, to evaluate the performance of the LM model against the horizontal distribution of ^{137}Cs deposition of the airborne radiological survey (NRA, 2012) (Fig. 4a) and surface air concentrations measured at Tsukuba (Fig. 1a). We selected this inventory because it is JAEA's most up-to-date version. Based on an integrated understanding of environmental radioactivity, atmospheric dispersion, and the nuclear reactors, the JAEA team has carefully established a series of inventories for about five years, staring with Chino et al. (2011), followed by Katata et al. (2012a), (2012b), Terada et al. (2012), and finally the current inventory (Katata et al., 2015), which is substantially improved compared to its predecessors.

Ongoing emissions during the study analysis period after the emergency situation, that is, January to December 2013, was obtained from the Tokyo Electric Power Co., Inc. (TEPCO) monthly mean emission flux from the reactor buildings (TEPCO, 2012; 2013; 2014a; 2014b; 2015). Because only the sum of ^{134}Cs and ^{137}Cs was provided, the fractions of these two isotopes were calculated based on their half-lives and the assumption that their activities were equal in March 2011 (e.g., Katata et al., 2015), as shown in Fig. 3. The values range from 10^5 to 10^7 Bq/h, but for simplicity we set a constant value of 10^6 Bq/h in the current simulation.

In August 2013, unexpected re-suspension associated with debris removal operations was reported by TEPCO (2014c) and NRA (2014) and the gross amount was 10^{10} – 10^{11} Bq of ^{137}Cs (TEPCO, 2014c, NRA, 2014, Steinhauser et al., 2015). The impact of this unexpected re-suspension is briefly discussed in Sect. 5.2 along with an additional finding, but this

Atmos. Chem. Phys. Discuss., doi:10.5194/acp-2016-270, 2016
Manuscript under review for journal Atmos. Chem. Phys.
Published: 25 April 2016

emission was not considered in the present LM simulation. In this study we focused on the ongoing emission, mostly from the natural environment, that is difficult to control.

3 Field observation

Details of the surface air activity concentration measurements can be found in Ishizuka et al. (2016) and Kinase et al. (2016) for Namie and Igarashi et al. (2015) for Tsukuba. At both sites, ambient aerosols were collected using a high-volume air sampler and ^{134}Cs and ^{137}Cs concentrations were obtained by γ-ray spectroscopy using a Ge semiconductor detector. The sampling intervals were 1 – 2 d (sometimes several days) at Namie and 1 w at Tsukuba for the analysis period of this study, the year 2013. The observations at Namie started on December 14, 2012, while those at Tsukuba started on March 31, 2003, before the FDNPP accident. In March 2011, the sampling interval was increased at Tsukuba to 6 h – 1 d and the data for these periods were used for the validation of LM and its parameters, as presented in Sect. 4.1.

The Namie site is located on the ground at Namie High School, Tsushima Campus, in the Tsushima district of Namie town in Fukushima prefecture, as shown in Table 1 and Fig. 1. Namie town extends from the Hamadori coastal area (denoted as C in Fig. 1) to the Abukuma highland area (B in Fig. 1). There are two sites in Namie town in the study. In order to distinguish the Tsushima Campus site in the highland area from the monitoring post site located in Omaru district in Namie town in the coastal area, the Tsushima site and the Omaru site are referred to as Namie (Tsushima) and Namie (Omaru), respectively. Note that, unless specifically referred to as Namie (Omaru), Namie without brackets indicates Namie (Tsushima) throughout this manuscript. The Tsukuba site is located on the premises of the Meteorological Research Institute (Table 1 and Fig. 1a).

Namie (Tsushima) was located in the DRZ (> 50 mSv/y, ~9.55 μSv/h[1]) and the observed ^{137}Cs deposition amount was 2,300 kBq/m^2 (Fig. 4a). The ambient gamma dose rate was 11.2 μSv/h on April 1, 2012 at the site and had dropped to 4.8 μSv/h on Feb 16, 2016, and at the HRZ level (20 – 50 mSv/y, 3.85 – 9.55 μSv/h). Tsukuba is located approximately 170 km southwest of FDNPP. The observed ^{137}Cs deposition amount was 21 kBq/m^2 (Fig. 4a), two

[1] Calculated by the following equation: Annual radiation exposure = (ambient dose rate – background dose rate (=0.04 μSv/h)) × (8 h + 0.4 × 16 h) × 365 d.

Atmos. Chem. Phys. Discuss., doi:10.5194/acp-2016-270, 2016
Manuscript under review for journal Atmos. Chem. Phys.
Published: 25 April 2016

orders of magnitude lower than at Namie and the dose rate has been below 0.1 μSv/h since 2012.

4 Results

Section 4.1 presents a validation of the LM model and the optimization of the model deposition parameters by using airborne observations (NRA, 2012) and the emission inventory of Katata et al. (2015) for the emergency situation of March 2011. Using the optimized ranges of model parameters validated in Sect. 4.1, the simulated re-suspension of ^{137}Cs from soil and forest, and emission from FDNPP, is presented in Sect. 4.2, and the budgets for re-suspension, transport, and re-deposition are presented in Sect. 4.3.

4.1 Model and parameter validation for the emergency situation (March 2011)

Figures 4 and 5 show the observed and simulated distribution of ^{137}Cs deposition in March 2011, and the scattergram comparing the observational and simulation results, respectively. In the simulation shown in the figures, the "reference" sets used for dry and wet deposition parameters, namely, the collection efficiency of aerosols using hydrometeors E_c (Eq. A2) and the dry deposition velocity over land v_d (Eq. A4), were 0.04 and 0.1 cm/s, respectively.

Since LM employs simple parameterizations for dry and wet deposition, as described in Appendix A, sensitivity tests were conducted for model validation, together with optimization of the deposition parameters. Table 2 summarizes the ranges of the deposition parameters for the sensitivity tests and the results of the ^{137}Cs budget and statistical measurements between the observations and the simulation.

The parameter E_c was 0.05 for the JMA dispersion model (JMA, 1998) but the targeted species are different. For example, volcanic ash (particles larger than 1 μm in diameter) used for the JMA model were generally larger than the carrier aerosols of ^{137}Cs (around 1 μm in diameter observed in the downwind area, Tsukuba, Kaneyasu et al. 2012, Adachi et al., 2013). Since the inertia of these smaller ^{137}Cs particles is likely to be smaller than that for volcanic ash, E_c could be smaller. The range of E_c was set as 0.02 – 0.06. The dry deposition velocity v_d was selected as 0.1 cm/s for ^{137}Cs in Furuno et al. (1999). The range for v_d was set as 0.05 to 0.15 in the present study.

Atmos. Chem. Phys. Discuss., doi:10.5194/acp-2016-270, 2016
Manuscript under review for journal Atmos. Chem. Phys.
Published: 25 April 2016

Atmospheric Chemistry and Physics Discussions

The emission inventory of Katata et al. (2015) amounted 14.1 PBq from March 12 to April 1, 2013. The simulated deposition over the model domain (138 – 143 °E, 34 – 39 °N) ranged from 3.4 – 4.7 PBq, which is approximately a quarter to one third of the emission from the FDNPP. Sixty percent of the total deposition occurred over land, for a total of 2.0 – 2.8 PBq, which is close to the observed value of 2.68 PBq, and the observed value is within the range of the sensitivity runs. Statistical measures such as the fractional bias *FB*, the correlation coefficient *R*, and *FAx* (fraction of the simulated values within a factor of *x*) are listed in Table 2. To find better combinations of (or to optimize) the dry and wet deposition parameters, sensitivity runs were screened based on the criteria $FA10 > 0.9$, $FA5 > 0.7$, $R > 0.75$, and an absolute value of $FB < 10\%$. After the screening, only one combination (E_c, v_d) = (0.04, 0.1 cm/s) was left, and thus this is referred to as the "reference" parameters. To evaluate the sensitivity (or uncertainty) of the re-suspension simulation for 2013 due to the deposition parameters, the range of the combination of parameters was set as (E_c, v_d) = (0.03 – 0.05, 0.05 – 0.1 cm/s) around the reference parameters (referred to as the "optimized range") by excluding the parameters with the worse performances. The ranges of the statistical measures of the optimized runs are listed in Table 2. *FB*, *R*, *FA2*, *FA5*, and *FA10* after the optimization had the ranges -0.18 – -0.036, 0.74 – 0.77, 0.26 – 0.30, 0.68 – 0.74, and 0.91 – 0.92, respectively. These statistical measures were comparable to those reported in previous multi-model comparison studies (*R*: 0.27 – 0.85, *FB*: -0.84 – 0.56, and *FA2*: 0.14 – 0.57, in SCJ, 2014 and Draxler et al., 2015). The current model is thus shown to be sufficiently credible for the budget analysis in this study, despite the simple parameterization and the low resolution in space (~11 km) and time (3 h).

Consistent with many previous studies, the simulated contribution of wet deposition was larger than that of dry deposition: the ratio of the amount of dry to wet deposition ranged from 0.12 – 0.23 for the optimized parameter ranges, indicating that the results were less sensitive to the dry deposition parameter. Generally speaking, *R* became higher as E_c became lower, whereas *FAx* became higher as E_c became higher for the various ranges of the sensitivity tests. Therefore, lower E_c did not meet the criteria of *FAx* and higher E_c did not meet the criteria of *R*. Consequently, after the optimization, the maximum values of the statistical measures were lower but the minimum values became higher, indicating that the optimization was successful in excluding the parameters with the worse performances (rather than selecting the best parameters). It should be noted here that the optimized deposition parameters are not necessarily physically true but rather are consistent with the available evidence. The results

Atmos. Chem. Phys. Discuss., doi:10.5194/acp-2016-270, 2016
Manuscript under review for journal Atmos. Chem. Phys.
Published: 25 April 2016

presented in this section indicate that the current LM simulation with these optimized parameters has the potential to reproduce consistent features of the radiocesium budget over the Tohoku and Kanto regions of Japan.

Figure 6 shows the temporal variation of simulated (red) and observed (black) ^{137}Cs concentrations at Tsukuba in March 2011. The model successfully reproduced the three major plumes arriving at Tsukuba on March 15-16, 20-21, and 28-30; a plume on March 23 only appeared in the simulation. The red shaded areas indicate the range of ^{137}Cs concentrations obtained when the simulations were run using the optimized parameter ranges E_c = 0.03 – 0.05 and v_d = 0.05 – 0.1 cm/s. Due to differences in the parameters, the surface air concentration could vary by approximately one order of magnitude in transported plumes that experienced wet scavenging along their pathway.

4.2 Re-suspension in 2013

Figure 7 shows the observed and daily mean simulated (with the reference parameters) surface air concentrations at Namie and Tsukuba for the year 2013. The red, green, and blue lines indicate re-suspension from soil, re-suspension from forest, and emission from the FDNPP reactor buildings, respectively. Note that the re-suspension flux due to the dust emission module (Ishizuka et al., 2016) is multiplied by 10 in this study by adjusting to the observation level at Namie in the cold season (January to March, October to December). Also note that the re-suspension coefficient r_{const} in Eq. (4) was set as 10^{-7}/h by adjusting to the observation level at Namie in the warm season (May to September). The emission flux reported by TEPCO varied from 10^5 to 10^7 Bq/h during the study period but we set it to 10^6 Bq/h for simplicity. We did not try to precisely adjust r_{const} to the observation by, for example, using inverse modeling, and instead we simply multiplied by power-of-ten values which are constant in time and space because (1) this aided straightforward interpretation of the simulation results by keeping the simulated variation as it was, and therefore (2) this provided simple but useful hints for understanding the re-suspension mechanisms, which remain unknown.

Using the dust emission module (which has a physical basis), ^{137}Cs flux re-suspended from soil could account for the level of the observed surface air concentration of ^{137}Cs at Namie in the cold season. Under the influence of the northwesterly winter monsoon, the surface wind speed is high over the contaminated area compared to in the summer (see Fig. 10). Note that

Atmos. Chem. Phys. Discuss., doi:10.5194/acp-2016-270, 2016
Manuscript under review for journal Atmos. Chem. Phys.
Published: 25 April 2016

the flux might be a maximum estimate since it does not consider land surface processes (such as soil moisture, snow cover, or migration of ^{137}Cs in the soil and biota) and decontamination, which could reduce the ^{137}Cs re-suspension flux. In contrast, in the warm season, the estimated flux significantly underestimated the observation by one to two orders of magnitude due to the weak surface wind, indicating that the dust emission process may not be the sole process involved in sustaining the air concentration of ^{137}Cs during this period. Introducing the ^{137}Cs re-suspension component from forest with a resuspension coefficient of 10^{-7}/h and a monthly variation in the green area fraction (derived from NDVI) could quantitatively account for the observed air concentration together with its seasonal variation at Namie. Even though both the simulated re-suspension from soil and forests reproduced the quantity and seasonal variation of the background concentration (in other words, concentrations originating from constantly presenting emissions) at Namie, sporadic peak events, such as the daily mean ^{137}Cs concentration exceeding 10 mBq/m^3 as observed in June and August at Namie, were not simulated. Some specific re-suspension events might occur within the premises of FDNPP or very close to this area on these days, as indicated later in Sect. 5.2. The simulated ^{137}Cs concentrations due to the monthly mean emission from the reactor buildings (=10^6 Bq/h) significantly underestimated the observed concentration by more than three orders of magnitude at Namie and by two orders of magnitude at Tsukuba. Even the maximum estimate of 10^7 Bq/h does not reach the observed level. The emission from FDNPP may not have been the sole process sustaining the air concentration of ^{137}Cs in 2013, supporting the discussion in Igarashi et al. (2015), which concluded that direct emission from the FDNPP played a minor role in the observed atmospheric radiocesium concentrations over Tsukuba during 2013-2014.

The observed air concentration of ^{137}Cs at Tsukuba was about one to two orders of magnitude lower than that at Namie. The simulated difference between the two sites in and out of the contaminated areas was consistent with the observed difference. This finding indicates that the current LM simulation provided consistent features of re-suspension, transport, and re-deposition in the Tohoku and Kanto regions of Japan of ^{137}Cs originating from Fukushima.

4.3 Budget analysis

Figure 8 illustrates the simulated (with the reference parameters) annual total re-suspension and re-deposition amounts of ^{137}Cs, together with their ratios to the observed deposition amount (Fig. 4a). The simulated areal total re-suspension amount was 1.01 TBq, which was

Atmos. Chem. Phys. Discuss., doi:10.5194/acp-2016-270, 2016
Manuscript under review for journal Atmos. Chem. Phys.
Published: 25 April 2016

equivalent to 0.037% of the total deposition amount, 2.68 PBq. The areal total re-deposition amount (with the reference parameters) was 0.22 TBq (0.18 – 0.23 TBq for the optimized range of the deposition parameters), corresponding to approximately 21.7 (17.8 – 22.8) % of the re-suspended amount deposited mainly in the Tohoku region, with the remainder being transported out of the region. Therefore, the regional mean rate in the decrease of the land surface ^{137}Cs concentration due to re-suspension was estimated to be 0.029 (0.029 – 0.031) %/y[2], equivalent to 7.9 (7.9 – 8.2) × 10^{-7} /d. The spatial distribution of the re-suspension and re-deposition ratio to the primary deposition ranged from 0.01 – 0.3% and 0.001 – 0.03%, respectively. The spatial distribution of the land surface ^{137}Cs deposition decay due to re-suspension ranged from 2.2×10^{-7} – 6.6×10^{-6} /d. Re-suspension therefore had a negligible effect on reducing land surface radioactive contamination.

5 Discussion

Seasonal variation of the surface activity concentration and its source contributions are extensively discussed in Sect. 5.1. A possible source of the observed sporadic peak events, which could not be reproduced by the simulation, is discussed in Sect. 5.2. Future issues are summarized in Sect. 5.3. The effects of other processes that were not considered in the model, such as land surface processes and decontamination, are discussed based on the dose rate measurements from the monitoring posts in Fukushima in Appendix C.

5.1 Seasonal variation and source contribution

The discussion in this section expands on that in Sect. 4.2. Figure 9 shows the same temporal variation as Fig. 7 but for simulated (using the optimized ranges of parameters) results for ^{137}Cs from dust and FDNPP in winter (January to March) and from forest and FDNPP in summer (June to August).

In the winter, the simulated trend for dust agreed well with the observed trend (Fig. 9a), and the surface air concentration during this period was positively correlated with the surface wind speed in both the simulation and the observations. There was a sporadic peak in the

[2] The amount re-suspended, excluding re-deposition (1.01 TBq minus 0.22 (0.18 – 0.23) TBq) for the year 2013, divided by the total deposition amount of 2.68 PBq.

Atmos. Chem. Phys. Discuss., doi:10.5194/acp-2016-270, 2016
Manuscript under review for journal Atmos. Chem. Phys.
Published: 25 April 2016

Atmospheric Chemistry and Physics Discussions

observational data of 6.7 mBq/m^3 from the March 17 at 13:00 local time (LT) to March 18 at 13:00 LT that could not be reproduced by the dust module, and this peak coincided with a plume arriving from FDNPP, as shown in Fig. 9c. The discrepancy between the observed peak and the dust simulation is likely due to underestimation of the simulation because the simulated dust peak reached an intensity of 4 – 5 mBq/m^3 in the winter, which is of the same order of magnitude as that of the observed peak. The observed peak could also be accounted for by specific re-suspension events on the order of 10^9 Bq/h (the left axis divided by the right axis multiplied by 10^6 Bq/h in Fig. 9c) if they occurred on the premises of FDNPP or close to the area. There are also two events exceeding 2 mBq/m^3, one in January and another in February. It is unlikely that the two peaks originated from the direct emission from FDNPP and likely that they originated from the dust emission because the observed peaks coincided with the simulated dust peaks (Fig. 9a) and not with the simulated peaks due to the FDNPP emission (Fig. 9c).

In the summer, the simulated quantity as well as the variation in the forest data agreed well with the observed data (Fig. 9b). Because there is only monthly variation in the simulated emission, the simulated daily trend solely originated from variations in the meteorological parameters (wind field, turbulent mixing, and wet scavenging). A significant peak of 60.4 mBq/m^3 is observed from August 14 at 13:00 LT to August 15 at 13:00 LT. This observed level was approximately two orders of magnitude larger than the simulated level and one to two orders of magnitude larger than the observed level for the other days in this period. Therefore, constant emission such as re-suspension from forest is less likely to be the origin of the peak. Because the observed peak and the simulated peak of ^{137}Cs from FDNPP coincided (Fig. 9d), the observed level could be accounted for by specific re-suspension events on the order of 10^{10} Bq/h either on the premises of FDNPP or close to the area. There have been several arguments that the observed peaks in August 2013 were associated with debris removal operations at FDNPP and this is discussed separately in Sect. 5.2.

Figure 10 illustrates the seasonal mean surface wind vector and surface air ^{137}Cs concentration (simulated using the reference parameters) due to (a) dust re-suspension in the winter and (b) forest re-suspension in the summer. Due to the prevailing northwesterly winter monsoon, ^{137}Cs was carried southeastward in the winter. In the summer, under the influence of the Pacific high pressure system, ^{137}Cs was carried inland. The monthly mean wind speed is high in winter and low in summer. The upper panels of Fig. 11 illustrate the observed and

Atmos. Chem. Phys. Discuss., doi:10.5194/acp-2016-270, 2016
Manuscript under review for journal Atmos. Chem. Phys.
Published: 25 April 2016

simulated (using the optimized ranges of parameters) total (from soil, forest, and FDNPP) ^{137}Cs concentration at Namie and Tsukuba. The time resolutions of the simulation are daily for Namie and weekly for Tsukuba to be consistent with the sampling intervals of the two respective sites. The simulation successfully reproduced the quantity and variation in the observed background concentration at Namie and Tsukuba but could not reproduce the sporadic peak events observed at Namie, as discussed above. The simulation also significantly underestimated the observations at Tsukuba from January to March, 2013. Due to the northwesterly monsoon (Fig. 10a), there was less air mass transported from FDNPP to Tsukuba in the winter (Fig. 12b) and therefore this underestimation is probably due specifically to underestimation of the simulated re-suspension. The lower panels of Fig. 11 show the relative contributions of ^{137}Cs from soil and forests at Namie and Tsukuba. The contribution from FDNPP was negligible throughout the year. At both sites, the contribution from dust was high (0.6 – 0.8) in the cold season and low (0.1 – 0.4) in the warm season.

Figure 12a shows the observed and simulated (with the reference parameters) monthly Namie to Tsukuba ^{137}Cs concentration ratios. The mean concentration ratio exceeded 100 in June and 200 in August due to the sporadic peak events. The monthly median would be relevant for comparing the background observation with the simulation results by considering only constant emissions. The values of the simulated concentration ratio and its seasonal variation agreed fairly well with the observed monthly median ratio: the observed and simulated annual means were 38.9 and 30.3, respectively. Fig. 12b shows the monthly mean simulated re-suspension source area contributions to the ^{137}Cs air concentration at Namie and Tsukuba. The re-suspension source area is defined as the model grid where the observed deposition amount exceeded 300 kBq/m^2 (Fig. 4a) and includes the Namie grid (2,300 kBq/m^2). Eighty to 90% of the ^{137}Cs air concentration at Namie originated from the source region, and there was no clear seasonal variation in the value. In contrast, Tsukuba is characterized as a downwind region and there was clear seasonal variation in the source contribution ratio: high in summer and low in winter, due to the summer and winter monsoons, as discussed above. Nonetheless, the highest value at Tsukuba was 0.4 in July, and so more than half of the ^{137}Cs concentration at Tsukuba originated locally or from areas other than the contaminated regions throughout the year. As shown in Figs. 11a and 11b, the variability in the simulated concentration at Tsukuba due to uncertainty in the deposition parameters was much larger than that at Namie. The differences in the variability indicated that the Namie and Tsukuba sites can be characterized as the source area and the downwind area, respectively: as the time

Atmos. Chem. Phys. Discuss., doi:10.5194/acp-2016-270, 2016
Manuscript under review for journal Atmos. Chem. Phys.
Published: 25 April 2016

required for the plume to move from the emission site to the observation site increases, the variability becomes larger due to the increased chance for the plume to experience dry and wet scavenging.

5.2 Possible source of sporadic peak events

There have been several scientific studies and governmental reports on the unexpected re-suspension from FDNPP in August 2013. The high dose rate alarm was activated on August 19 within the premises of FDNPP associated with the debris removal operation. Matsunami et al. (2016) related the radiocesium contamination of brown rice in Fukushima in 2013 to this operation, whereas MAFF (2015) denied any association. The NRA estimated the ^{137}Cs emission rate during the debris removal operation as 6.7×10^{10} Bq/h and the cumulative amount as 1.1×10^{11} Bq (NRA, 2014). TEPCO (2014c) estimated the emission rate during the operation as 5.8×10^{10} – 1.2×10^{11} Bq/h and the cumulative amount as 1.3 – 2.6×10^{11} Bq. Steinhauser et al. (2015) estimated the gross amount as 2.8×10^{11} Bq using measurements of weekly air filter sampling and monthly deposition, and a numerical simulation. Their estimates are of the similar order of magnitude as our estimate (10^{10} Bq/h, see Sect. 5.1) but the dates are different: our observed peak was earlier than the reported removal operation.

Our daily sampling showed a peak concentration (60.4 mBq/m^3) from August 14 at 13:00 LT to August 15 at 13:00 LT before the reported operation, but did not detect high concentrations in the August 19 (0.33 mBq/h for August 18 at 13:00 LT to August 19 at 13:00 LT and 1.2 mBq/h for August 19 at 13:00 to August 20 at 13:00 LT). Figure 13 shows the forward trajectories predicted by the LM (statistical locations of LPs) starting from FDNPP on August 14 (left) and August 19 (right). The sky-blue lines and red dashed circles indicate areas containing approximately two-thirds of the LPs within 1 km AGL: the extent of the area reflects horizontal and vertical atmospheric diffusion. The highest dose rate peaks were observed from 13:50 LT to 14:10 LT on August 19 at 2.8 – 8.3 km north and north-northwest of FDNPP on the leeward side, as reported by Fukushima prefecture (https://www.pref.fukushima.lg.jp/download/1/20130827moni.pdf.pdf, last access: March 11, 2016). The forward trajectories on August 19 indicated that plumes during the debris removal operation traveled north-northwest to north of FDNPP (Figs 13b and 13d), rather than toward the west-northwest where the Namie site is located. On August 14, on the other hand, plumes were transported toward the west (starting at 12 LT, Fig 13a), and then to the north (starting at 15 LT, Fig. 13c) due to fast changes in wind direction, resulting in the simulated peak

Atmos. Chem. Phys. Discuss., doi:10.5194/acp-2016-270, 2016
Manuscript under review for journal Atmos. Chem. Phys.
Published: 25 April 2016

concentration shown in Fig. 9d during this period. Our simulation and observations together indicated that the same order of magnitude of ^{137}Cs emission occurred on August 14 – 15 and on August 19. Alarm activation was not reported on August 14 – 15 but debris removal operation was also conducted on August 14 and 16 (MAFF, 2015).

5.3 Future issues

Issues that remain to be resolved in future research are summarized as follows:

1. Re-suspension from the biota could be predominant in the warm season but the re-suspension sources as well as mechanisms remain essentially unknown. Further study is needed to understand the mechanism based on field experiments and numerical simulations.
2. The current estimation could account for the measured background concentration (0.1 – 1 mBq/m^3) but could not reproduce the observed sporadic peak concentration (1 – 10 mBq/m^3) at the Namie site. Further study is needed to identify the cause.
3. The dust flux module has been validated at a single location. The module could be extended to be applicable to various land use and soil texture conditions.
4. The current estimation was based on a single model simulation. Variability in multi-model simulations is rather large (SCJ, 2014; Draxler et al., 2015) and therefore multi-model assessment will be indispensable for long-term re-suspension analysis.

6 Conclusions

The long-term effect of ^{137}Cs re-suspension from contaminated soil and biota due to the Fukushima nuclear accident has been quantitatively assessed using a numerical simulation, a field experiment on dust emission in the contaminated area (Namie, Fukushima), and air concentration measurements inside (Namie) and outside (Tsukuba, Ibaraki) of the area. The re-suspension mechanism remains unknown. We therefore utilized observational data obtained both inside and outside the contaminated area, together with 3D numerical simulation, to provide a robust budget analysis of the re-suspension, transport, and re-deposition of ^{137}Cs in the eastern part (the Tohoku and Kanto regions) of Japan. Our findings are summarized as follows:

Atmos. Chem. Phys. Discuss., doi:10.5194/acp-2016-270, 2016
Manuscript under review for journal Atmos. Chem. Phys.
Published: 25 April 2016

Atmospheric Chemistry and Physics Discussions

1. Optimization of the deposition parameters of the LM for simulating the emergency situation of March 2011, using aircraft observation data (NRA, 2012) and the prescribed emission inventory (Katata et al., 2015), provided 0.1 (0.05 – 0.1) cm/s for a dry deposition velocity over land and 0.04 (0.03 – 0.05) for a hydrometeor collection efficiency for aerosols. The optimized (or validated) ranges of the deposition parameters were applied to long-term re-suspension assessment for the year 2013.

2. Using the dust emission module (Ishizuka et al., 2016), which was developed based on physical parameters, simulated ^{137}Cs re-suspension from soil multiplied by 10 accounted for the observed ^{137}Cs surface air concentration measured at Namie in only the cold season; the module underestimated the ^{137}Cs concentration by one to two orders of magnitude in the warm season. Introducing re-suspension from forest using a constant re-suspension coefficient of 10^{-7} /h and monthly green area fraction could quantitatively account for the observed concentration together with its seasonal variation. The contribution from additional emission from the reactor buildings of FDNPP (10^{6} Bq/h) was negligible throughout the year and underestimated the observed air concentration by two to three orders of magnitude at both observation sites.

3. At Namie and Tsukuba, the simulated contribution of re-suspension from soil was high (0.6 – 0.8) in the cold season and low (0.1 – 0.4) in the warm season; the remaining contribution was from forest and was low in winter and high in summer. The contribution of the re-suspension from the source area (where the aircraft-observed deposition exceeded 300 kBq/m^2) to the air concentration at Namie was 0.8 – 0.9 throughout the year, while that at Tsukuba varied from 0.1 to 0.4, and was high in the summer and low in the winter.

4. The simulated total re-suspended amount for the whole region was 1.01 TBq, equivalent to 0.037% of the aircraft-observed total deposition amount of 2.68 PBq. The total re-deposition was 0.18 – 0.23 TBq, equivalent to 17.8 – 22.8% of the total re-suspended amount: the rest of the ^{137}Cs was transported out of the model domain. The spatial distribution of the decreasing rate of land surface ^{137}Cs due to re-suspension ranged from 2.2×10^{-7} – 6.6×10^{-6} /d. The first order decrease rate of the ambient gamma dose rate in Fukushima prefecture ranged from 5.2 – 12.1×10^{-4} /d. By subtracting the radioactive decay rate of 3.0 – 4.2 $\times10^{-4}$ /d, the ground radioactivity decay due to land surface processes, decontamination, and re-suspension was found to range from 1.0 – 7.9×10^{-4} /d.

Atmos. Chem. Phys. Discuss., doi:10.5194/acp-2016-270, 2016
Manuscript under review for journal Atmos. Chem. Phys.
Published: 25 April 2016

Atmospheric Chemistry and Physics Discussions

The estimated re-suspension rate was two to three orders of magnitude lower than the decrease in rate due to the other processes, showing that re-suspension contributed negligibly toward reducing ground radioactivity.

Appendix A: Model description

The current study employs a Lagrangian type model for the simulation of emission (either point sources or areal sources), horizontal and vertical diffusion and advection, gravitational settling, dry and wet depositions, and radioactive decay in the air. As described in Sect. 2.1, the current Lagrangian Model (LM) uses simple parameterizations for dry and wet deposition schemes for computational efficiency, so long-term assessment and parameter sweep experiments are easily feasible. The source code for the model is open with the BSD 3-Clause License and is available on the web (http://157.82.240.167/~dl3/, in Japanese, last access: 12 February 2016).

The coordinate system of the model is horizontal for longitude and latitude and vertical for pressure level, consistent with meteorological analysis data commonly used. The model can be driven only by fundamental meteorological parameters such as temperature, humidity, 3D wind field, geopotential height, and surface precipitation provided by meteorological analysis data such as GPV-MSM. The model does not need to drive meteorological models to predict detailed meteorological variables such as cloud microphysics, turbulence quantities, and surface variables. Since the temporal and spatial resolution of the meteorological analysis is not very high (e.g., 3 h and ~11 km for GPV-MSM, respectively), linear interpolation is conducted in time and space. Alternatively, higher temporal and spatial resolution can be achieved by using a meteorological model. Furthermore, although currently not implemented, detailed variables predicted by a meteorological model can be used for more accurate predictions of turbulent diffusion, surface flux, and dry and wet deposition.

In the LM model, LPs are released constantly in time but the initial activity of LPs (Bq/LP) differs accordingly to the emission flux (Bq/h). The initial positions of LPs were randomly distributed within a fixed volume (or line) of plume centered at a point emission source such as FDNPP for the primary emission case simulation, or randomly distributed within a horizontal model grid for the areal emission cases (such as re-suspension from soil and forest). LPs do not disappear unless transported across lateral and upper boundaries or if they reach the surface layer due to gravitational settling (technically, gravitational settling velocity in the

Atmos. Chem. Phys. Discuss., doi:10.5194/acp-2016-270, 2016
Manuscript under review for journal Atmos. Chem. Phys.
Published: 25 April 2016

surface layer is included in the dry deposition velocity). The other processes, such as dry deposition, wet deposition and radioactive decay, do not decrease the number of LPs but do decrease the radioactivity carried by LPs because LPs represent an air mass rather than an actual particle, except in the case of gravitational settling. The lowest level permitted for the position of LPs is set as 2 m AGL and LPs going down across the level due to vertical turbulent motion will rebound at the level and go up. An LP whose radioactivity is smaller than a preset value, i.e., 10^{-10} Bq, due to deposition or radioactive decay will disappear from the computation to maintain computational efficiency, since the cost of the computation is proportional to the number of LPs in the model domain. To output the model results, the LP fields are converted to Eulerian concentration (Bq/m^3) and deposition (Bq/m^2) fields on a prescribed coordinate system of grids. In Lagrangian type models, the spatial resolution of tracer emission, concentration, and deposition fields can be set independent of each other and with the spatial resolution of meteorological fields. In the current implementation of the LM, the coordinate system of meteorological fields and radioactivity fields is horizontal for common (longitude and latitude) but vertical for different (pressure level and meters AGL, respectively).

The horizontal and vertical diffusion calculation followed JMA (2008), using the horizontal diffusion scheme of Uliasz (1990) with a constant horizontal diffusivity of 5.864×10^4 m^2/s and using a vertical diffusivity calculated based on Louis et al. (1982) (see Eqs. 8.1.8 through 8.1.15 of JMA (2008) for details). The incremental change in location of an LP δx (y, z) after a time step δt was defined as

$$\delta x = \frac{\mathrm{d}x}{\mathrm{d}t} G \delta t \ , \qquad \text{(A1)}$$

where G is the normalized Gaussian random number (average = 0, standard deviation = 1). δt is set large enough for computational efficiency but without violating the Courant-Friedrichs-Lewy (CFL) condition of $\delta t < 0.5\ U/\Delta x$, where U (or $\mathrm{d}x/\mathrm{d}t$) is the typical wind speed and Δx is the grid size in the direction of U. However, the selection of δt is not critical because every time step prior to applying Eq. (A1) time splitting is made so that the split step always satisfies the CFL condition.

The wet scavenging rate Λ_{wet} (/s) is simply parameterized as a function of the surface precipitation rate P (mm/s) as

Atmos. Chem. Phys. Discuss., doi:10.5194/acp-2016-270, 2016
Manuscript under review for journal Atmos. Chem. Phys.
Published: 25 April 2016

Atmospheric Chemistry and Physics Discussions

$$\Lambda_{wet} = \frac{3}{4}\frac{E_c(a_m, r_m)}{a_m}P, \quad \text{(A2)}$$

where E_c is the collection efficiency of aerosols by the hydrometeor, and a_m and r_m are the mean radii of the hydrometeor and aerosols, respectively (JMA, 2008). Empirically, a_m is characterized by P as

$$a_m = 0.35P^{0.25}. \quad \text{(A3)}$$

JMA (2008) uses 0.05 for E_c. In the current study, instead of explicitly predicting E_c, its range was set for the sensitivity tests as listed in Table 2.

Conceptually, Eq. (A2) is the formulation for the washout process, i.e., the collection of aerosols by the settling hydrometeor particles such as rain and snow. a_m and E_c should differ for rain and snow, but common parameters are used in the current simulation. Also, Eq. (A2) is not applicable for the rainout process, since this process—cloud condensation nuclei or ice nuclei activation and deposition via subsequent cloud microphysical processes— is totally different from the washout process. Because meteorological models were not utilized in this study and thus only relative humidity and surface precipitation rate are available and no cloud microphysical information (such as hydrometeors mixing ratio in each model grid) is available, Eq. (A2) is applied for all the LPs located above the grid with P. In order to partly account for the rainout process, Eq. (A2) is not applied to LPs in a grid, where the relative humidity is lower than the minimum value, set as 95% in the simulation.

The dry deposition velocity v_d (m/s) of aerosols (or gases) is conventionally formulated, using an electrical analogy, as an inverse of the summation of resistances (s/m) representing turbulent diffusion in the surface layer, Brownian diffusion (or molecular diffusion for gases), interaction with the land surface (soil, water and vegetation), and gravitational settling for aerosols (e.g., Wesely and Hicks, 2000). Therefore, v_d is a function of height as well as of turbulent flux and surface conditions. Nevertheless, v_d is set as constant in the simulation, but the height dependency of v_d is considered in the dry scavenging rate Λ_{dry} (/s), following Furuno et al. (1999) as

$$\Lambda_{\mathrm{dry}} = \frac{2}{z_{srf}}\left(1 - \frac{z}{z_{srf}}\right)v_d, \quad \text{(A4)}$$

where z is the height of the LP (m AGL) and z_{srf} is the surface layer height set as 100 m AGL in the study. Instead of explicitly predicting v_d, its range was set at around 0.1 cm/s, a typical

Atmos. Chem. Phys. Discuss., doi:10.5194/acp-2016-270, 2016
Manuscript under review for journal Atmos. Chem. Phys.
Published: 25 April 2016

speed for a range of aerosols around 1 μm in diameter, for the sensitivity tests, as listed in Table 2. The value of v_d is applied over land, whereas v_d over the ocean is multiplied by 0.1, because v_d over a flat surface is approximately one and two orders of magnitude smaller than v_d over short vegetation such as grass and tall vegetation such as forest, respectively (e.g., Petroff and Zhang, 2010).

Appendix B: Statistical accuracy of the current simulation setting

Because the statistical error of Lagrangian simulation is inversely proportional to the square of the number of LPs, the statistical accuracy of the current simulation setting was evaluated using the following measures (relative errors of quantities of the sensitivity runs to those of the reference run):

$$E_{con}(x,y) = \frac{\left|C_{sens}(x,y) - C_{ref}(x,y)\right|}{C_{ref}(x,y)}, \quad \text{(B1)}$$

$$E_{dep}(x,y) = \frac{\left|D_{sens}(x,y) - D_{ref}(x,y)\right|}{D_{ref}(x,y)}, \quad \text{(B2)}$$

where x and y indicate grid points on the longitudinal and latitudinal axes, respectively. C_{sens} and D_{sens} indicate temporal mean surface concentrations (Bq/m^3) and temporal cumulative depositions (Bq/m^2) of the sensitivity runs, respectively. C_{ref} and D_{ref} are the same as C_{sens} and D_{sens} but for the reference run. E_{con} and E_{dep} were sampled only at grids where $C_{ref}(x,y)$ and $D_{ref}(x,y)$ are greater than their areal mean values, respectively.

B.1 Point source case

The number emission rate of LPs, N_{LP}, was set as 32,000 /h (=N_{LP_ref}) for a point source emission case such as the primary emission in March 2011 and additional emission from the reactor buildings in 2013. The median values together with the 25th and 75th percentile values of E_{con} and E_{dep} of the sensitivity runs (sensitivity to deposition parameters and sensitivity to N_{LP}) against the reference run are listed on the top half rows of Table B1. Both E_{con} and E_{dep} of N_{LP_ref} ×4 were significantly lower than those for the deposition parameters sensitivity run. This result indicates that 32,000 /h for N_{LP} was sufficient to allow a statistically significant simulation for the purpose of this study, as shown in Figs. 4 and 5: the

Atmos. Chem. Phys. Discuss., doi:10.5194/acp-2016-270, 2016
Manuscript under review for journal Atmos. Chem. Phys.
Published: 25 April 2016

Atmospheric Chemistry and Physics Discussions

difference in concentration and deposition due to the deposition parameters was much larger than the difference due to model uncertainty in N_{LP}. E_{con} and E_{dep} of $N_{LP\_ref} \times 0.25$ (which are also smaller than those of the deposition parameters sensitivity run) are larger than those of $N_{LP\_ref} \times 4$, indicating fairly well accuracy convergence of the LM model.

B.2 Areal emission case

N_{LP_ref} was 16 /h/grid for the areal emission case simulating re-suspension from soil and forests in 2013. The lower half of Table B1 is the same as the upper half except for the areal emission case (re-suspension from forest). Both E_{con} and E_{dep} of $N_{LP\_ref} \times 4$ were much lower than those for the deposition parameters sensitivity run, indicating that 16 /h/grid supports a statistically significant simulation for the purpose of this study, as shown in Figs. 7 - 12. Usually, Eulerian-type models are appropriate for solving areal emission problems—Lagrangian-type models require many more LPs for areal emission cases compared to point source cases and thus become computationally too expensive. In the case of this simulation, especially for the concentration, sensitivity to deposition parameters was much more significant than sensitivity to model uncertainty in N_{LP} using the sufficiently small number of $N_{LP\_ref} = 16$ /h/grid. E_{con} and E_{dep} of $N_{LP\_ref} \times 4$ are smaller than those of $N_{LP\_ref} \times 0.25$, indicating fairly accuracy convergence of the LM model.

Appendix C: Land surface processes, decontamination, and dust emission suppression due to snow cover

Figure C1 presents the time series of ambient gamma dose rates measured at the monitoring posts in Fukushima prefecture indicated in Fig. 1b. The data were obtained from the Nuclear Regulation Authority (NRA), Japan website (http://radioactivity.nsr.go.jp/map/ja/index.html, last access: Feb 16, 2016). A total of six, two of the monitoring posts from three geographical areas (Hamadori coastal area, Abukuma highland area, and Nakadori valley area), were selected. There are tens to hundreds of monitoring posts in each municipality (village, town, and city) in Fukushima prefecture. We selected a monitoring post in each municipality by applying the following conditions: a post showing the highest dose rate of all posts in the municipality at the time of downloading (around 11:00 a.m., December 28, 2015), data are available since April 1, 2012, and the instruments are situated 100 cm above the ground.

Atmos. Chem. Phys. Discuss., doi:10.5194/acp-2016-270, 2016
Manuscript under review for journal Atmos. Chem. Phys.
Published: 25 April 2016

Atmospheric Chemistry and Physics Discussions

The government of Japan designated the evacuation-directed zones as a Difficult-to-Return zone (DRZ) (> 50 mSv/y; 9.55 μSv/h), a Habitation-Restricted Zone (HRZ) (20 – 50 mSv/y; 3.85 – 9.55 μSv/h), and a zone being prepared to have the evacuation directive lifted (< 20 mSv/y; 3.85 μSv/h), in April 2012 (METI, 2012). The two sites in the Hamadori area, Okuma and Namie (Omaru), have been designated DRZ (13.6 and 11.8 μSv/h on December 28, 2015). The dose rates at the two sites in the Abukuma area, Iitate and Kawamata, dropped below the HRZ level during the analysis period in this study (1.17 and 0.521 μSv/h on December 28, 2015). The dose rates in the Nakadori area are below 1 μSv/h (0.242 and 0.201 μSv/h on December 28, 2015).

The dose rate significantly dropped when the ground was covered with snow, in January and December 2013 in Hamadori and Nakadori, and from January to early March and December 2013 in Abukuma (the elevation of Abukuma is 500 – 1,000 m and higher than Hamadori and Nakadori). Snow cover suppresses re-suspension due to dust emission. Namie (Tsushima) is located in Abukuma and the ground was covered with snow until early March (Ishizuka et al., 2016). The observed air concentration of ^{137}Cs at Namie (Tsushima) was correlated with the wind speed in the winter from January to March, indicating that re-suspension during the period was mechanically induced. In the winter, dust re-suspension from outside Abukuma, such as from Hamadori and Nakadori, or from land surface where the snow cover was partly melted due to solar radiation, might be the dominant source contributing to the ^{137}Cs surface air concentration at Namie (Tsushima) when the ground was covered with snow.

The first order decreasing rates fitted by the least-square approximation for the period without snow cover, May to October 2012 and 2013, are presented in Fig. C1. The rates ranged from 5.2 – 12.1 $\times 10^{-4}$ /d. The monthly mean radioactive decay rates of total radiocesium (^{134}Cs + ^{137}Cs), determined by assuming that the activities of ^{134}Cs and ^{137}Cs were equivalent in March 2011, were 4.2×10^{-4} /d and 3.0×10^{-4} /d in April 2012 and March 2014, respectively, due to the difference in half-life of ^{134}Cs and ^{137}Cs (2.07 y and 30.1 y, respectively). By assuming that the gamma dose rate primarily originated to radiation from the land surface radiocesium, the radioactive decay accounted for 35 – 50% of the decreasing rate of total ground radioactivity; the exception was Shirakawa, where radioactive decay accounted for 55 – 80% of the decrease. In other words, 50 – 65% of the ground radioactivity decrease was likely due to land surface processes, decontamination, and re-suspension to air. As discussed in Sect. 4.3, the estimated decreasing rate due to re-suspension was 2.2×10^{-7} – 6.6×10^{-6} /d, which is two to

Atmos. Chem. Phys. Discuss., doi:10.5194/acp-2016-270, 2016
Manuscript under review for journal Atmos. Chem. Phys.
Published: 25 April 2016

three orders of magnitude smaller than the decreasing rates due to the other processes (10^{-4} – 10^{-3} /d).

It is difficult to distinguish the contributions of land surface processes and decontamination. By subtracting the radioactive decay rate ($3.0 – 4.2\times10^{-4}$ /d) and the decreasing rate due to re-suspension ($2.2\times10^{-7} – 6.6\times10^{-6}$ /d) from the gross decreasing rate ($5.2 – 12.1 \times10^{-4}$ /d), the estimated decreasing rates due to land surface processes and decontamination ranged from $1.0 – 7.9\times10^{-4}$ /d. Matsuda et al. (2015) summarized the depth profiles of radiocesium in soil at more than 80 locations in Fukushima, including Hamadori, Abukuma, and Nakadori. They found that the radiocesium levels have been slowly migrating downward with rates ranging from 1.7 – 9.6 kg/m^2/y (equivalent to 1.1 – 6.0 mm/y for a dust particle density of 2650 kg/m^3 and a porosity of 0.4 m^3/m^3, for example). The downward migration resulted in decreasing the air dose rate due to incremental soil layers blocking radiation, but the downward migration rate has not been quantitatively related to the decrease in the air dose rate. This quantitative relationship needs to be assessed for the quantitative and individual assessment of land surface processes and decontamination effects.

Acknowledgements

This research was mainly supported by Grants-in-Aid for Scientific Research on Innovative Areas (24110002 and 20110003) from the Ministry of Education, Culture, Sports, Science and Technology (MEXT), and partly supported by the Japan Society for the Promotion of Science (JSPS), Ministère des Affaires Étrangères et du Développement International (MAEDI) under the Japan-France Integrated Action Program (SAKURA), and by KAKENHI Grant Numbers 15K16121, 24340115, and 26310201 from MEXT. Partial expenses were covered by the Japanese Radioactivity Survey from the NRA, Japan. The authors are grateful for useful discussions with and comments from Prof. Yuichi Moriguchi of University of Tokyo, Prof. Hiromi Yamazawa of Nagoya University, and Dr. Haruo Tsuruta of Remote Sensing Technology Center of Japan (RESTEC). The LM was developed by MI, CY, and MK.

References

Adachi, K., Kajino, M., Zaizen, Y., and Igarashi, Y.: Emission of spherical cesium-bearing particles from an early stage of the Fukushima nuclear accident, Scientific Report, 3, 2554, doi:10.1038/srep02554, 2013.

Chino, M., Nakayama, H., Nagai, H., Terada, H., Katata, G., and Yamazawa, H.: Preliminary estimation of release amounts of ^{131}I and ^{137}Cs accidentally discharged from the Fukushima Daiichi nuclear power plant into atmosphere, J. Nucl. Sci. Technol., 48, 1129-1134, 2011.

Danielache, S. O., Yoshikawa, C., Priyadarshi, A., Takemura, T., Ueno, Y., Thiemens, M. H.,and Yoshida, N.: An estimation of the radioactive ^{35}S emitted into the atmospheric from the Fukushima Daiichi Nuclear Power Plant by using a numerical simulation global transport, Geochemical Journal, 46, 355-339, 2012.

Danielache, S. O., Yoshikawa, C., Kajino, M., Itou, S., Kakeya, W., Yoshida, N., Igarashi, Y.: Radioactive ^{35}S emitted from the Fukushima Nuclear Power Plan studied by a modified regional model, 2016, manuscript in preparation.

Draxler, R., Arnold, D., Chino, M., Galmarini, S., Hort, M., Jones, A., Leadbetter, S., Malo, A., Maurer, C., Rolph, G., Saito, K., Servranckx, R., Shimbori, T., Solazzo, E., Wotawa, G.: World Meteorological Organization's model simulations of the radionuclide dispersion and deposition from the Fukushima Daiichi nuclear power plant accident, J. Environ. Radioact., 139, 172-184, 2015.

Furuno, A., Chino, M., and Yamazawa, H.: Worldwide version of System of Prediction of Environmental Emergency Dose Information (WSPEEDI) Model Code (II) – Three-dimensional Atmospheric Dispersion Model for Synoptic Scale: GEARN, JAERI-Data/Code 99-044, Japan Atomic Energy Research Institute, Japan (in Japanese), 68 pp., 1999.

Garger, E.K., Paretzke, H.G., Tschiersch, J.: Measurement of resuspended aerosol in the Chernobyl area. Part III: size distribution and dry deposition velocity of radioactive particles during anthropogenic enhanced resuspension, Radiation and Environmental Biophysics 37, 201-208, 1998.

Garger, E. K., Kuzmenko, Y. I., Sickinger, S., Tschiersch, J.: Prediction of the ^{137}Cs activity concentration in the atmospheric surface layer of the Chernobyl exclusion zone, J. Environ. Radioact., 110, 53-8, 2012.

Girard, S., Mallet, V., Korsakissok, I., and Mathieu, A.: Emulation and Sobl' sensitivity analysis of an atmospheric dispersion model applied to the Fukushima nuclear accident, J. Geophys. Res., 2016, in press.

Groëll J., Quélo, D., and Mathieu, A.: Sensitivity analysis of the modelled deposition of ^{137}Cs on the Japanese land following the Fukushima accident, Int. J. of Environment and Pollution, 55, 67-75, 2014.

Gutman, G., and Ignatov, A.: The derivation of green vegetation fraction from NOAA/AVHRR data for use in numerical weather prediction models, Int. J. Remote Sens., 19, 1533-1543, 1998.

Hatano, Y., and Hatano N.: Formula for the resuspension factor and estimation of the date of surface contamination, Atmos. Environ., 37, 3475-3480, 2003.

Hirao, S., Yamazawa, H., Nagae, T.: Estimation of release rate of iodine-131 and cesium-137 from the Fukushima Daiichi nuclear power plant, J. Nucl. Sci. Technol., 50, 139-147, doi:10.1080/00223131.2013.757454, 2013.

Holländer, W., Garger, E.: Contamination of Surface by Resuspended Material. ECP–1, Final Report, Rep. EUR 16527. Office for Official Publications of the European Communities, Luxembourg, 1996.

Hososhima, M. and Kaneyasu, N.: Altitude-dependent distribution of ambient gamma dose rates in mountainous area of Japan caused by the Fukushima nuclear accident. Environ. Sci. Technolo., 49(6), 3341-3348, 2015.

Igarashi, Y., Kajino, M., Zaizen, Y., Adachi, K., and Mikami, M.: Atmospheric radioactivity over Tsukuba, Japan: a summary of three years of observations after the FDNPP accident, Progress in Earth and Planetary Science, 2:44, doi:10.1186/s40645-015-0066-1, 2015.

Ishizuka, M, Mikami, M., Tanaka, T. Y., Igarashi, Y., Kita, K., Yamada, Y., Yoshida, N., Toyoda, S., Satou, Y., Kinase, T., Ninomiya, K., Shinohara, A.: Use of a size-resolved 1-D resuspension scheme to evaluation resuspended radioactive material associated with mineral dust particles from the ground surface, J. Environ. Radioact., 13pp., doi:10.1016/j.jenvrad.2015.12.023, 2016, in press.

JMA: Japan Meteorological Agency's Non-Hydrostatic Model II, *Suuchi Yohoka Hokoku Bessatsu* (Additional Volume to Report of Numerical Prediction Division) 54, 265 pp., 2008 (in Japanese).

Kaneyasu, N., Ohashi, H., Suzuki, F., Okada, T., and Ikemori, F.: Sulfate aerosol as a potential transport medium of radiocesium from the Fukushima nuclear accident, Environ. Sci. Technol. 46, 5720-5726, 2012.

Katata, G., Terada, H., Nagai, H., and Chino, M.: Numerical reconstruction of high dose rate zones due to the Fukushima Daiichi Nuclear Power Plant accident, J. Environ. Radioact., 111, 2-12, 2012a.

Katata, G., Ota, M., Terada, H., Chino, M., and Nagai, H.: Atmospheric discharge and dispersion of radionuclides during the Fukushima Dai-ichi Nuclear Power Plant accident, Part I: Source term estimation and local-scale atmospheric dispersion in early phase of the accident, J. Environ. Radioact, 109, 103-113, doi:10.1016/j.jenvrad.2012.02.006, 2012b.

Katata, G., Chino, M., Kobayashi, T., Terada, H., Ota, M., Nagai, H., Kajino, M., Draxler, R., Hort, M. C., Malo, A., Torii, T., and Sanada, Y.: Detailed source term estimation of the atmospheric release for the Fukushima Daiichi Nuclear Power Station accident by coupling simulations of an atmospheric dispersion model with an improved deposition scheme and oceanic dispersion model. Atmos. Chem. Phys., 15, 1029-1070, 2015.

Kinase, T., Kita, K. Igarashi, Y., Adachi, K., Ninomiya, K., Shinohara, A., Okochi, H., Ogata, Y., Ishizuka, M., Toyoda, S., Yamada, K., Yoshida, N., Zaizen, Y., Mikami, M., Demizu, H., and Onda, Y.: Seasonal variation in activity concentration of atmospheric ^{134,137}Cs and their possibile resuspension host aerosol observed at Tsuahima and Yamakiya, Fukushima, 2016, in preparation.

Loosmore, G. A., Hunt, J. R.: Dust resuspension without saltation, J. Geophys. Res., 105(D16), 20,663-20,671, doi:10.1029/2000JD900271, 2002.

Louis, J. F., Tiedtke, M., Geleyn, J. F.: A short history of the PBL parameterization at ECMWF, *Workshop on planetary boundary layer parameterization. ECMWF*, 59-80, 1982.

MAFF (Ministry of Agriculture, Forestry and Fisheries), Fukushima Prefecture, Tohoku Agricultural Research Center, National Institute for Agro-Environmental Sciences: Investigation of the cause for brown rice exceeding the allowable radiocesium concentration,

available at http://www.maff.go.jp/j/kanbo/joho/saigai/fukusima/pdf/150526_youin_chosa.pdf (last access, 10 March, 2016), 2015 (in Japanese).

Masson, O., Baeza, A., Bieringer, J., Brudecki., Bucci, S., Cappai, M., Carvalho, F. P., Connan, O., Cosma, C., Dalheimer, A., Didier, D., Depuydt, G., De Geer, L. E., De Vismes, A., Gini, L., Groppi, F., Gudnason, K., Gurriaran, R., Hainz, D., Halldórsson, O., Hammond, D., Hanley, O., Holey, K., Homoki, Zs., Ioannidou, A., Isajenko, K., Jankovic, M., Katzlberger, C., Kettunen, M., Kierepko, R., Kontro, R., Kwakman, P. J. M., Lecomte, M., Leon Vintro, L., Leppänen, A.-P., Lind, B., Lujaniene, G., Mc Ginnity, P., Mc Mahon, C., Malá, H., Manenti, S., Manolopoulou, M., Mattila., A., Mauring., A., Mietelski, J. W., Moller, B., Nielsen, S. P., Nikolic, J., Overwater, R. M. W., Pálsson, S. E., Papastefanou, C., Penev, I., Pham, M. K., Povinec, P. P., Ramebäck, H., Reis, M. C., Ringer, W., Rodriguez, A., Rulik, P., Saey, P. R. J., Samsonov, V., Schlosser, C., Sgorbati, G., Silobritiene, B. V., Söderström, C., Sogni, R., Solier, L., Sonck, M., Steinhauser, G., Steinkopff, T., Steinmann, P., Stoulos, S., Sýkora, I., Todorovic, D., Tooloutalaie, N., Tositti, L., Tschiersch, J., Ugron, A., Vagena, E., Vargas, A., Wershofen, H., Zhukova, O. Tracking of Airborne Radionuclides from the Damaged Fukushima Dai-Ichi Nuclear Reactors by European Networks. Environ. Sci. Technol. 2011, 45 (18), 7670-7677, 2011.

Masson, O., Ringer, W., Malá, H., Rulik, P., Dlugosz-Lisiecka, M., Eleftheriadis, K., Meisenberg, O., De Vismes-Ott, A., and Gensdarmes, F.: Size distribution of airborne radionuclides from the Fukushima Nuclear Accident at several places in Europe, Environ. Sci. Technol., 47, 10995-11003, 2013.

Matsunami H., Murakami, T., Fujiwara, H., and Shinano, T.: Evaluation of the cause of unexplained radiocaesium contamination of brown rice in Fukushima in 2013 using autoradiography and gamma-ray spectrometry, Scientific Report, 6, 20386, doi:10.1038/srep20386, 2016.

METI (Ministry of Economy, Trade and Industry): Convention on Nuclear Safety National Report of Japan for the Second Extraordinary Meeting, July 2012, Government of Japan, available at www.meti.go.jp/english/press/2012/pdf/0705_01b.pdf (last access: 19 February, 2016), 2012.

Miller, D. A. and White, R. A.: A conterminous United States multi-layer soil characteristics data set for regional climate and hydrology modeling, Earth Interactions, 2, 1-26, 1998.

Matsuda, N., Mikami, S., Shimoura, S., Takahashi, J., Nakano, M., Shimada, K., Uno, K., Hagiwara, S., and Saito, K.: Depth profiles of radioactive cesium in soil using a scraper plate over a wide area surrounding the Fukushima Dai-ichi Nuclear Power Plant, Japan., 139, J. Environ. Radioact., 427-434, 2015.

Morino, Y., Ohara, T., and Nishizawa, M.: Atmospheric behavior, deposition, and budget of radioactive materials from the Fukushima Daiichi nuclear power plant in March 2011, Geophys. Res. Lett. 38, doi:10.1029/2011GL048689, 2011.

Morino, Y., Ohara, T., Watanabe, S., Hayashi, S., and Nishizawa, M.: Episode analysis of deposition of radiocesium from the Fukushima Daiichi Nuclear Power Plant accident, Environ. Sci. Technol., 47, 2314-2322, 2013.

NRA (Nuclear Regulation Authority): Airborne Monitoring Results in each prefecture, available at: http://radioactivity.nsr.go.jp/en/list/203/list-1.html (last access: 25 December 2015), 2012.

NRA: Assessment of radionuclide emission involved in the debris removal operations for reactor 3; Handout for the 28th meeting on the supervision of a specific nuclear facility, available at http://www.nsr.go.jp/data/000051154.pdf (last access, 10 March 2016), 2014 (in Japanese).

Ohmori, Y., Kajikawa, M., Nishida, S., Tanaka, N., Kobayashi, N. I., Tanoi, K., Furukawa, and J., Fujiwara, T.: The effect of fertilization on cesium concentration of rice grown in a paddy field in Fukushima Prefecture in 2011 and 2012, J. Plant Res., 127, 1, 67-71, 2014.

Oura, Y., Ebihara, M., Tsuruta, H., Nakajima, T., Ohara, T., Ishimoto, M., Sawahata, H., Katsumura, Y., and Nitta, W.: A database of hourly atmospheric concentrations of radiocesium (^{134}Cs and ^{137}Cs) in suspended particulate matter collected in March 2011 at 99 air pollution monitoring stations in Eastern Japan, Journal of Nuclear and Radiochemical Sciences, 15(2), 15-26, 2015.

Petroff, A. and Zhang L.: Development and validation of a size-resolved particle dry deposition scheme for application in aerosol transport models, Geosci. Model Dev. 3, 753-769, 2010.

Pöhlker C., Wiedemann, K. T., Sinha, B., Shiraiwa, M., Gunthe, S. S., Smith, M., Su, H., Artaxo, P., Chen, Q., Cheng, Y., Elbert, W., Gilles, M. K., Kilcoyne, A. L. D., Moffet, R. C>,

Weigand, M., Matin, S. T., Pöschl, U., and Andreae, M. O.: Biogenic potassium salt particles as seeds for secondary organic aerosol in the Amazon, Science, 337, 1075-1078, 2012.

Quérel, A., Roustan, Y., Quélo, D., and Benoit, J. -P.: Hints to discriminate the choice of wet deposition models applied to an accidental radioactive release, Int. J. of Environment and Pollution, in review.

Saito, K., Shimbori, T., and Draxler, R.: JMA's regional atmospheric transport model calculations for the WMO technical task team on meteorological analyses for Fukushima Daiichi Nuclear Power Plant accident, J. Environ. Raioact., 139, 185-199, 2015.

Saunier, O., Mathieu, A., Didier, D., Tombette, M., Quelo, D., Winiarek, V., and Bocquet, M.: An inverse modeling method to assess the source term of the Fukushima Nuclear Power Plant accident using gamma dose rate observations, Atmos. Chem. Phys., 13, 11403-11421, doi:10.5194/acp-13-11403-2013, 2013.

SCJ (Science Council of Japan): A review of the model comparison of transportation and deposition of radioactive materials released to the environment as a result of the Tokyo Electric Power Company's Fukushima Daiichi Nuclear Power Plant accident, available at http://www.scj.go.jp/ja/info/kohyo/pdf/kohyo-22-h140902-e1.pdf (last access: 22 February 2016), 2014.

Sekiyama, T. T., Kunii, M., Kajino, M., and Shimbori, T.: Horizontal resolution dependence of atmospheric simulations of the Fukushima nuclear accident using 15-km, 3-km, and 500-m grid models, J. Meteor. Soc. Japan, 93, 49-64, 2015.

Sekiyama, T. T., Kajino, M., and Kunii, M.: Ensemble dispersion simulation of a point-source radioactive aerosol using a square root Kalman filter, J. Geophys. Res., 2016, in review.

Skamarock, W. C., Klemp, J. B., Dudhia, J., Grill, D. O., Barker, D. M., Duda, M. G., Huang, X. Y., Wang, W., and Powers, J. G.: A description of the advanced research WRF version 3, Tech. Note, NCAR/TN~475+STR, 125 pp., Natl. Cent. For Atmos. Res., Boulder, Colo., 2008.

Steinhauser, G., Niisoe, T., Harada, K. H., Shozugawa, K., Schneider, S., Synal, H.-A, Walther, C., Christl, M., Nanba, K., Ishikawa, H., and Koizumi, A: Post-accident sporadic releases of airborne radionuclides from the Fukushima Daiichi Nuclear Power Plant Site, Environ. Sci. Technol., 49, 14028-14035, doi:10.1021/acs.est.5b03155, 2015.

Stohl, A. Seibert, P., Wotawa, G., Arnold, D., Burkhart, J. F., Eckhardt, S., Tapia, C., Vargas, A., and Yasunari, T. J.: Xenon-133 and caesium-137 releases into the atmosphere from the Fukushima Dai-ichi nuclear power plant: determination of the source term, atmospheric dispersion, and deposition. Atmos. Chem. Phys., 12, 2313-2343, 2012.

TEPCO (Tokyo Electric Power Co., Inc.): Estimation of additional emissions from nuclear reactor buildings (30 July 2012), available at: http://www.tepco.co.jp/nu/fukushima-np/roadmap/images/m120730_05-j.pdf (last access: 25 December 2015), 2012 (in Japanese).

TEPCO: Estimation of the additional emission from nuclear reactor buildings (30 May 2013), available at: http://www.tepco.co.jp/nu/fukushima-np/roadmap/images/d130530_05-j.pdf (last access: 25 December 2015), 2013 (in Japanese).

TEPCO: Estimation of the additional emission from nuclear reactor buildings (27 March 2014), available at: http://www.tepco.co.jp/nu/fukushima-np/roadmap/images/d140327_06-j.pdf (last access: 25 December 2015), 2014a (in Japanese).

TEPCO: Estimation of the additional emission from nuclear reactor buildings (25 December 2014), available at: http://www.tepco.co.jp/nu/fukushima-np/roadmap/images/d141225_08-j.pdf (last access: 25 December 2015), 2014b (in Japanese).

TEPCO: Estimation of radioactive material released during debris removal operations at reactor unit 3 of the Fukushima Daiichi Nuclear Power Plant in August 2013, available at http://www.nsr.go.jp/data/000051136.pdf (last access: 10 March, 2016), 2014c (in Japanese).

TEPCO: Estimation of the additional emission from nuclear reactor buildings (9 October 2015), available at: http://www.tepco.co.jp/life/custom/faq/images/d151109_11-j.pdf (last access: 25 December 2015), 2015 (in Japanese).

Terada, H., Katata, G., Chino, M., and Nagai, H.: Atmospheric discharge and dispersion of radionuclides during the Fukushima Dai-ichi Nuclear Power Plant accident, Part II: Verification of the source term and analysis of regional-scale atmospheric dispersion, J. Environ. Radioact., 112, 141-154, 2012.

Tsuruta, H., Oura, Y., Ebihara, M., Ohara, T., and Nakajima, T.: First retrieval of hourly atmospheric radionuclides just after the Fukushima accident by analysing filter-tapes of operational air pollution monitoring stations, Scientific Reports, 4, 6717, doi:10.1038/srep06717, 2014.

Uliasz, M.: Development of the mesoscale dispersion modelling system using personal computers. Part I: Models and computer implementation. Z. Meteor., 40, 110-120, 1990.

Wesely, M. L. and Hicks, B. B.: A review of the current status of knowledge on dry deposition, Atmos. Environ., 34, 2261-2282, 2000.

Winiarek, V., Bocquet, M., Saunier, O., and Mathieu, A.: Estimation of errors in the inverse modeling of accidental release of atmospheric pollutant: Application to the reconstruction of the cesium-137 and iodine-131 source terms from the Fukushima Daiichi power plant, J. Geophys. Res., 117, D05122, 16 pp, doi:10.1029/2011JD016932, 2012.

Winiarek, V., Bocquet, M., Duhanyan, N., Roustan, Y., Saunier, O., and Mathieu, A.: Estimation of the caesium-137 source term from the Fukushima Daiichi nuclear power plant using a consistent joint assimilation of air concentration and deposition observations, Atmos. Environ., 82, 268-279, 2014.

Yasunari, T. J., Stohl A., Hayano R. S., Burkhart J. F., Eckhardt S., and Yasunari T.: Cesium-137 deposition and contamination of Japanese soils due to the Fukushima nuclear accident. Proc. Natl. Acad. Sci., 108, 19530-19534, 2011.

Yumimoto, K., Mirno, Y., Ohara, T., Oura, Y., Ebihara, M., Tsuruta, H., and Nakajima, T.: Inverse modeling of the 137Cs source term of the Fukushima Dai-ichi Nuclear Power Plant accident constrained by a deposition map monitored by aircraft, J. Environ. Radioact., 2016, in review.

Atmos. Chem. Phys. Discuss., doi:10.5194/acp-2016-270, 2016
Manuscript under review for journal Atmos. Chem. Phys.
Published: 25 April 2016

Atmospheric Chemistry and Physics Discussions

Table 1. The observation sites and monitoring posts used to provide data for this study.

Name	Location	Description
Observation sites		
Namie (Tsushima)	140.7683 °E, 37.5621 °N	Namie High School, Tsushima Campus[1]
Tsukuba	140.1254 °E, 36.0551 °N	Meteorological Research Institute
Monitoring posts		
Okuma	140.9969 °E, 37.4163 °N	Ottozawa 3 Community Center[2]
Namie (Omaru)	140.9296 °E, 37.4665 °N	Omaru Multipurpose Community Center[3]
Iitate	140.7385 °E, 37.6772 °N	Iitate Junior High School[4]
Kawamata	140.6979 °E, 37.5836 °N	Yamakiya Otsu 8 Community Firehouse[5]
Fukushima	140.4765 °E, 37.6870 °N	Fukushima-Minami Fire Department
Shirakawa	140.1904 °E, 37.1241 °N	Takayama-Kita Park

1. Original location (now moved to Nihonmatsu city).
2. Ottozawa San-ku Chiku Shukaijo (in Japanese)
3. Omaru Tamokuteki Shukaijo (in Japanese)
4. Original location (now moved to Fukushima city).
5. Yamakiya Otsu Hachi-ku Community Shoubou Center (in Japanese)

Atmos. Chem. Phys. Discuss., doi:10.5194/acp-2016-270, 2016
Manuscript under review for journal Atmos. Chem. Phys.
Published: 25 April 2016

Atmospheric Chemistry and Physics Discussions

Table 2. ^{137}Cs budget and statistical analysis for the comparison of observed and simulated deposition data for March 2011.

	E_c[a] (-)	v_d[b] (cm/s)	D_{all}[c] (PBq)	D_{land}[d] (PBq)	FB[e]	R[f]	$FA2$[g]	$FA5$[h]
Sensitivity test								
Range	0.02 – 0.06	0.05 – 0.15	3.4 – 4.7	2.0 – 2.8	-0.25 – 0.00050	0.73 – 0.78	0.25 – 0.30	0.63 – 0.77
Optimization used for the re-suspension analysis for 2013								
Reference	0.04	0.10	4.2	2.5	-6.2	0.75	0.28	0.74
Optimized range	0.03 – 0.05	0.05 – 0.10	3.7 – 4.3	2.2 – 2.6	-0.18 – -0.036	0.74 – 0.77	0.26 – 0.30	0.68 – 0.74
Reference values								
Observed deposition over land D_{obs} (NRA, 2012)				2.68 PBq				
Emission amount (Katata et al., 2015)				14.1 PBq				

[a] Collection efficiency, see Eq. (A2) [b] Dry deposition velocity over land, see Eq. (A4). [c] Simulated deposition amount over the whole model domain. [d] Simulated deposition amount only over land. [e] Fractional bias between D_{land} and $D_{obs.}$ [f] Correlation coefficient between each grid cell of the observed and simulated deposition (linear vs. linear). [g] Fraction of simulated values within a factor of 2 of the observed values. [h] Fraction of simulated values within a factor of 5 of the observed values. [f, g, h] Compared only at grids where the observed values are greater than 10 kBq/m^2.

Atmos. Chem. Phys. Discuss., doi:10.5194/acp-2016-270, 2016
Manuscript under review for journal Atmos. Chem. Phys.
Published: 25 April 2016

Atmospheric Chemistry and Physics Discussions

Table B1. Statistical measures of temporal mean ^{137}Cs surface concentration (E_{con}) and cumulative deposition (E_{dep}) of the sensitivity runs against the reference run for (top) the point source case and (bottom) the areal emission case.

	Number emission rate of LP, N_{LP} (/h/grid)	E_c [a] (-)	v_d [b] (cm/s)	Median (25th – 75th percentile) of E_{con} [c] (%)	Median (25th – 75th percentile) of E_{dep} [d] (%)
Point source case, March 2011					
Reference run	32,000	0.04	0.01	-	-
Sensitivity runs					
Deposition parameters	32,000	0.03 – 0.05	0.05 – 0.01	2.7 (0.37 – 5.0)	7.5 (3.6 – 13)
$N_{LP\_ref} \times 4$	128,000	0.04	0.01	0.51 (0.21 – 0.96)	0.72 (0.32 – 1.5)
$N_{LP\_ref} \times 0.25$	8,000	0.04	0.01	0.95 (0.39-1.8)	1.6 (0.73 – 2.9)
Areal emission case, 2013 (re-suspension from forest)					
Reference run	16	0.04	0.10	-	-
Sensitivity runs					
Deposition parameters	16	0.03 – 0.05	0.05 – 0.01	7.3 (2.6 – 13)	7.7 (3.6 – 17)
$N_{LP\_ref} \times 4$	64	0.04	0.10	0.39 (0.17 – 0.78)	2.0 (1.3 – 2.6)
$N_{LP\_ref} \times 0.25$	4	0.04	0.10	0.78 (0.34-1.5)	2.3 (1.5 – 3.1)

[a] Collection efficiency, see Eq. (A2). [b] Dry deposition velocity over land, see Eq. (A4). [c] Relative errors of temporal mean surface concentration at each grid cell of the sensitivity run to that of the reference run, see Eq. (B1). [d] same as E_{con} but for cumulative deposition, see Eq. (B2).

Atmos. Chem. Phys. Discuss., doi:10.5194/acp-2016-270, 2016
Manuscript under review for journal Atmos. Chem. Phys.
Published: 25 April 2016

Atmospheric Chemistry and Physics Discussions

1

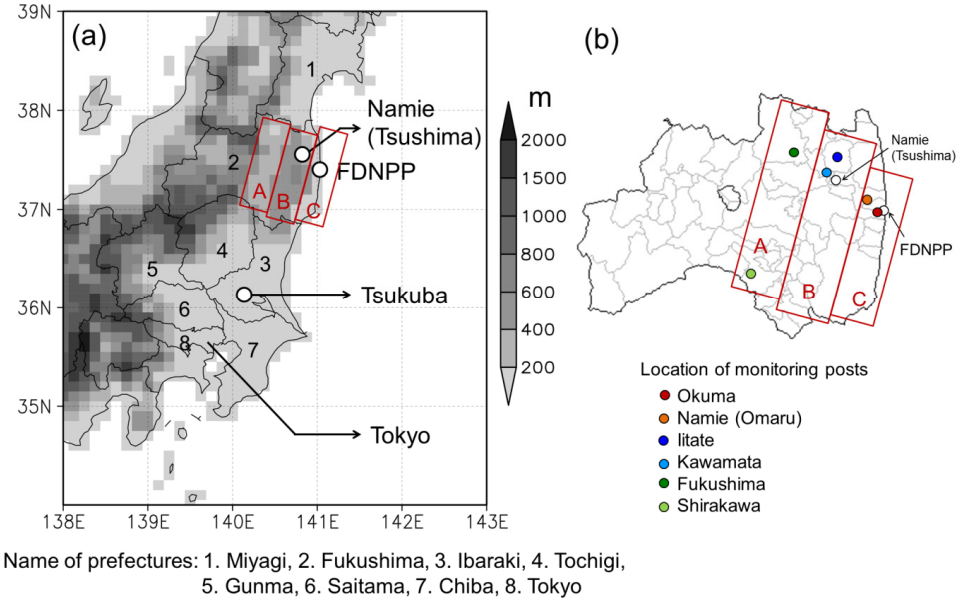

2

3 Figure 1. (a) The model domain showing the model terrestrial elevation, observation sites, and
4 other locations described in the study. The linear distances from FDNPP to Namie (Tsushima
5 district, Namie town), Tsukuba and Tokyo are approximately 30 km, 170 km, and 220 km,
6 respectively. The numbers denote prefectures: 1. Miyagi, 2. Fukushima, 3. Ibaraki, 4. Tochigi,
7 5. Gunma, 6. Saitama, 7. Chiba, and 8. Tokyo. (b) Fukushima prefecture and (colored circles)
8 the locations (village, town, or city name) of monitoring posts used in this study (see Fig. C1).
9 The letters in both (a) and (b) denote the name of the area based on geographical features: A.
10 Nakadori valley, B. Abukuma highland, and C. Hamadori coastal area.

11

Atmos. Chem. Phys. Discuss., doi:10.5194/acp-2016-270, 2016
Manuscript under review for journal Atmos. Chem. Phys.
Published: 25 April 2016

Atmospheric Chemistry and Physics Discussions

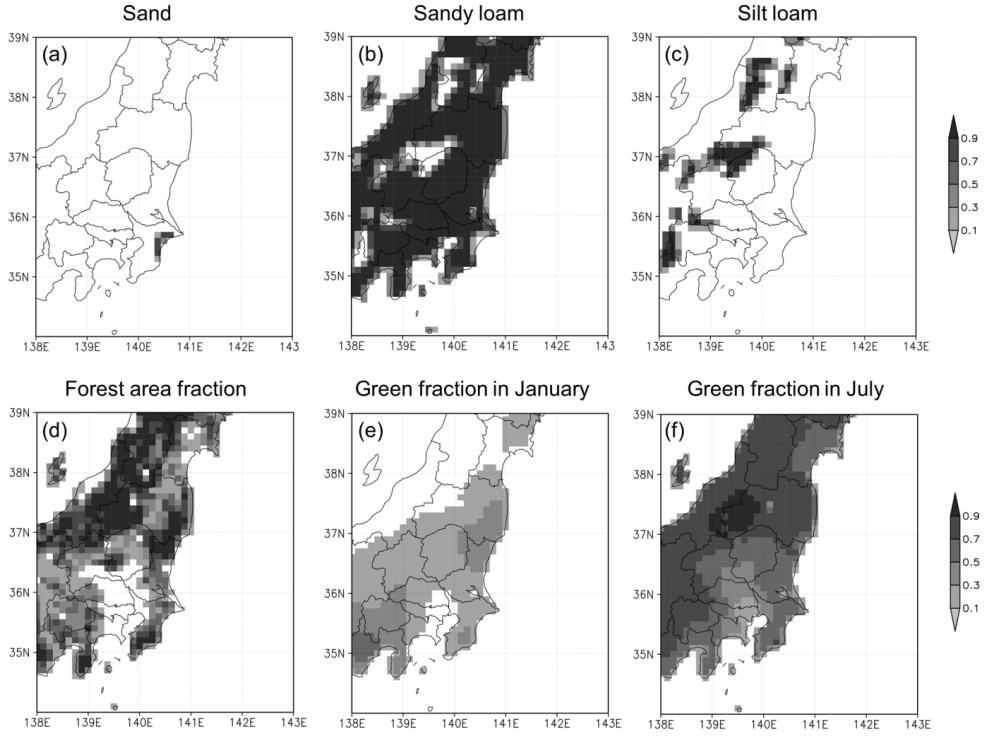

Figure 2. The areal fractions of (a)-(c) soil texture and (d)-(f) land use category used for the boundary conditions of the simulation.

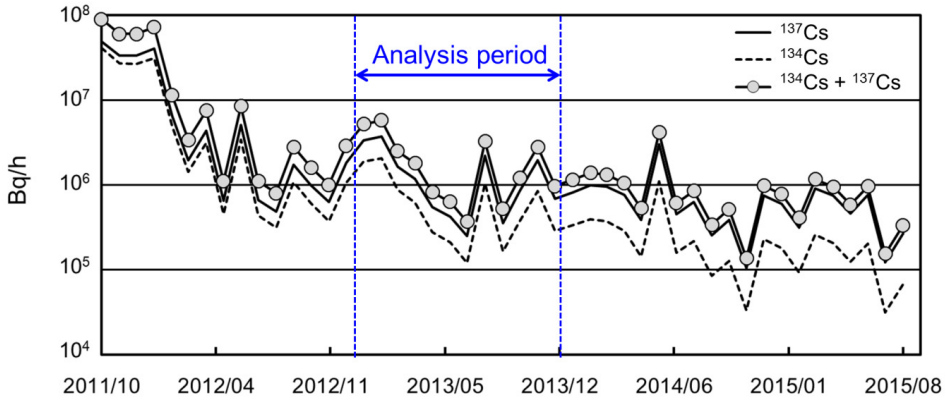

Figure 3. Monthly mean emission flux of radiocesium released from the reactor buildings of FDNPP from October 2011 to August 2015 as estimated by TEPCO (TEPCO, 2012-2015).

Atmos. Chem. Phys. Discuss., doi:10.5194/acp-2016-270, 2016
Manuscript under review for journal Atmos. Chem. Phys.
Published: 25 April 2016

Atmospheric Chemistry and Physics Discussions

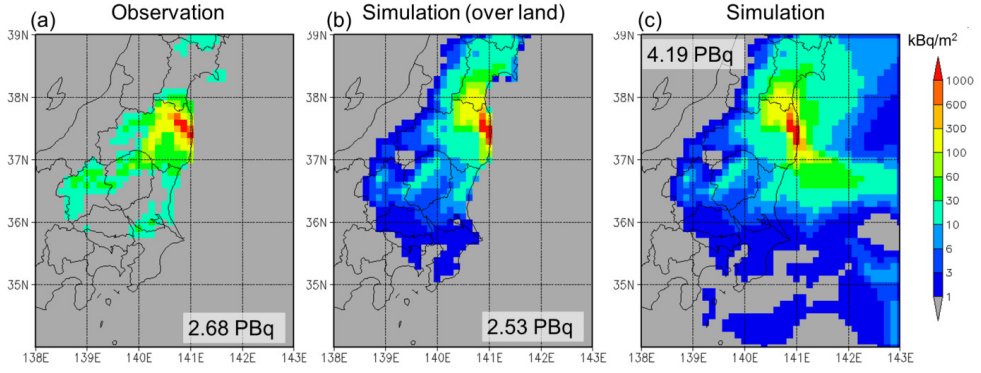

Figure 4. (a) Aircraft observation and (b), (c) simulation of ^{137}Cs deposition depicted (b) only over land and (c) for the whole domain (kBq/m^2). The observation was interpolated to the model grid (Δlongitude = 0.125° and Δlatitude = 0.1°). A decay correction for the observation was made for March - May 2012, varied depending on the region. The simulation provided a cumulative value from March 12 to April 1, 2011. The total activities are presented as numbers. The color scales are the same for (a) – (c) but observed values are not depicted below the detection limit, 10 kBq/m^2. The deposition parameters of the simulation in the figure are E_c = 0.04 and v_d = 0.1 cm/s.

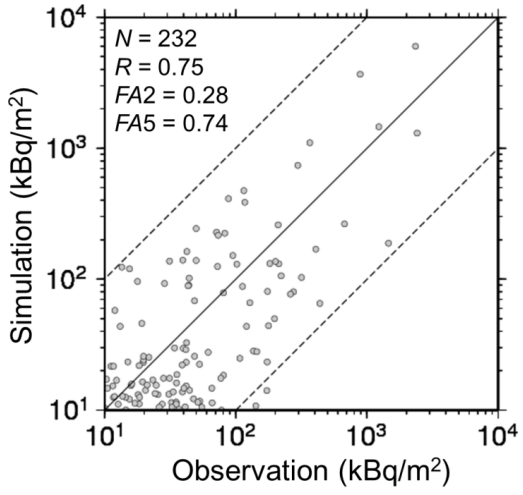

Figure 5. Scattergram between the observational data and the simulation results for ^{137}Cs deposition (kBq/m^2). The deposition parameters of the simulation in the figure are E_c = 0.04 and v_d = 0.1 cm/s. *N* indicates the number of samples, and the statistical measures *R*, *FA2*, and *FA5* are described in Table 2.

Atmos. Chem. Phys. Discuss., doi:10.5194/acp-2016-270, 2016
Manuscript under review for journal Atmos. Chem. Phys.
Published: 25 April 2016

Atmospheric Chemistry and Physics Discussions

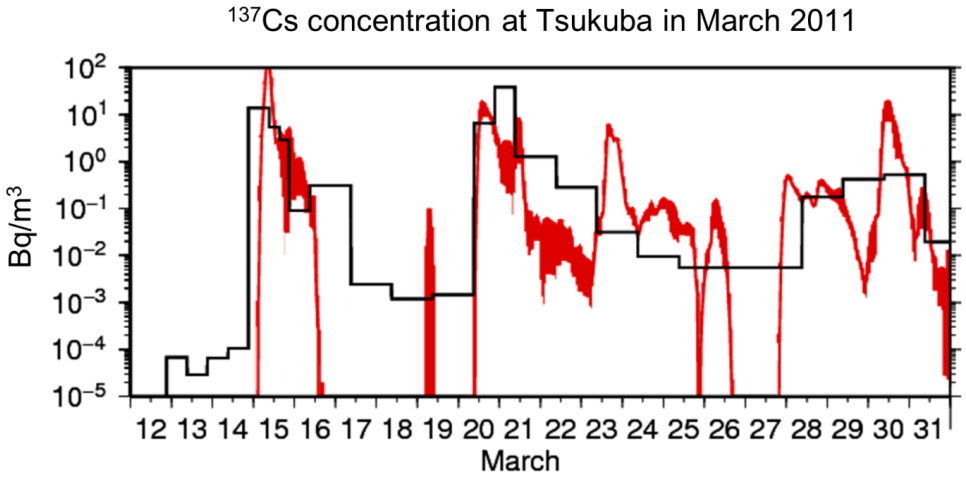

Figure 6. Time series of the surface activity concentration of (black) observed and (red) simulated ^{137}Cs concentrations at Tsukuba from March 12 to April 1, 2011 (Bq/m^3). The red shaded areas indicate the range of ^{137}Cs concentrations obtained when the simulations were run using the optimized parameter ranges E_c = 0.03 – 0.05 and v_d = 0.05 – 0.1 cm/s.

Atmos. Chem. Phys. Discuss., doi:10.5194/acp-2016-270, 2016
Manuscript under review for journal Atmos. Chem. Phys.
Published: 25 April 2016

Atmospheric Chemistry and Physics Discussions

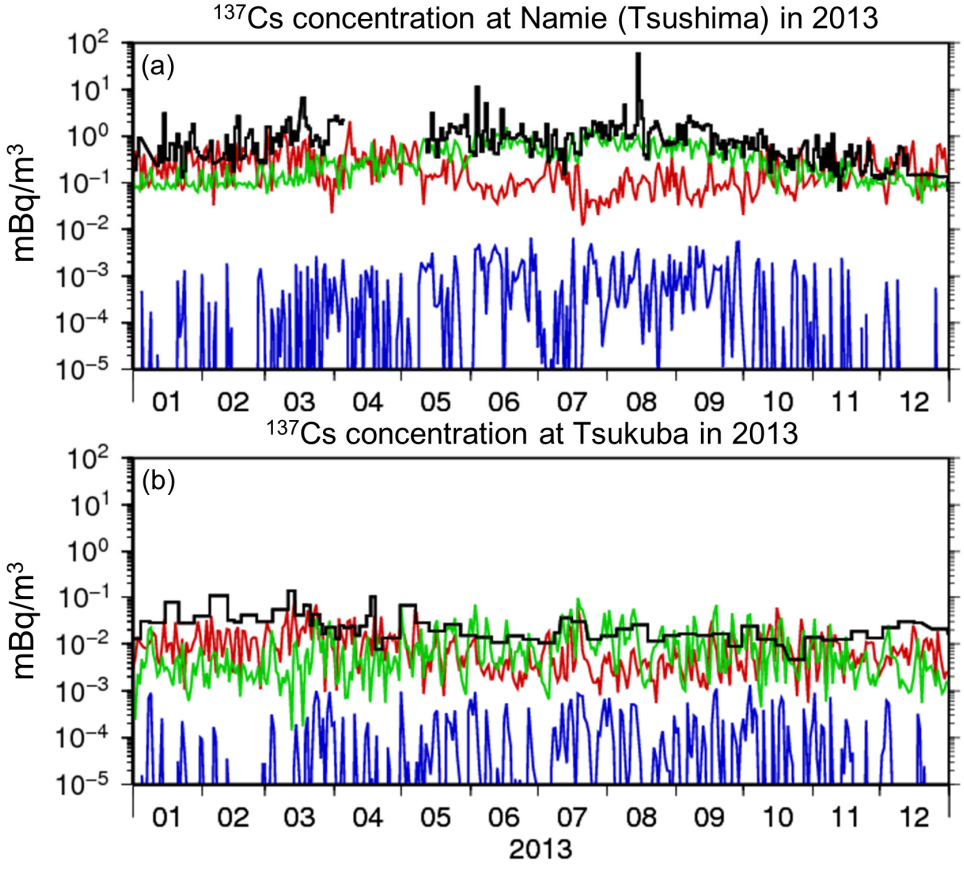

Figure 7. Time series of the surface air concentration of (black) observed ^{137}Cs and (colors) simulated daily ^{137}Cs levels at (a) Namie and (b) Tsukuba. The colored lines indicate simulated ^{137}Cs concentrations due to (red) re-suspension from soil using the scheme given in Ishizuka et al. (2016) (10 times), (green) re-suspension from forest with a re-suspension rate of 10^{-7} /h, and (blue) emission from the FDNPP reactor buildings with a constant emission rate of 10^{6} Bq/h. The deposition parameters of the simulation in the figure are E_c = 0.04 and v_d = 0.1 cm/s.

Atmos. Chem. Phys. Discuss., doi:10.5194/acp-2016-270, 2016
Manuscript under review for journal Atmos. Chem. Phys.
Published: 25 April 2016

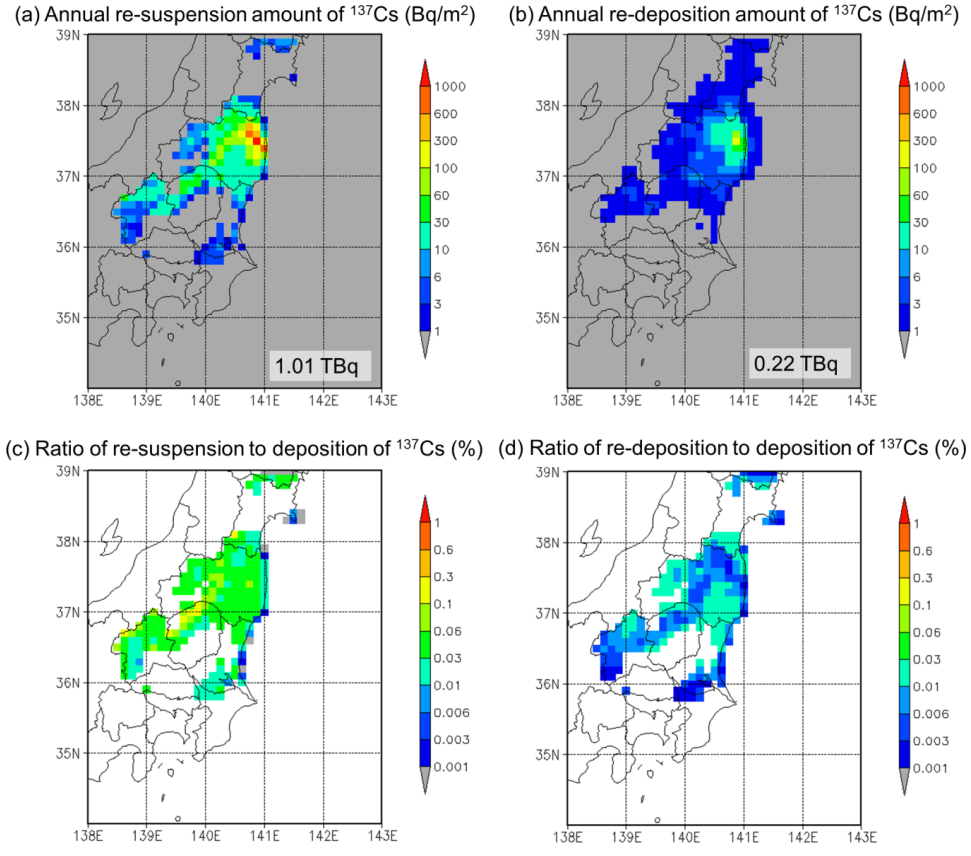

Figure 8. (a) Annual total re-suspension amounts of ^{137}Cs and (b) the re-deposition amounts. The total activities are presented as numbers. Ratios of the re-suspension and the re-deposition to the observed ^{137}Cs deposition amounts are also shown in (c) and (d), respectively. The deposition parameters of the simulation in the figure are E_c = 0.04 and V_d = 0.1 cm/s.

Atmos. Chem. Phys. Discuss., doi:10.5194/acp-2016-270, 2016
Manuscript under review for journal Atmos. Chem. Phys.
Published: 25 April 2016

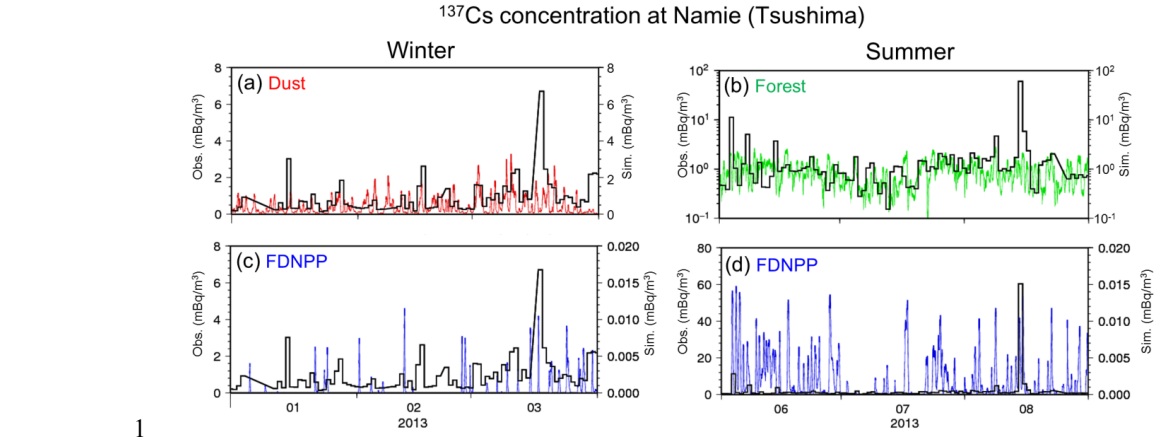

Figure 9. Time series of (black) the observed and (colors) the simulated ^{137}Cs surface air concentration at Namie (a, c) in winter from January to March and (b, d) in summer from June to August, 2013. The colors of the lines are the same as in Fig. 7 but the time variation is hourly. The shaded areas indicate the range of ^{137}Cs concentrations obtained when the simulations were run using the optimized parameter ranges E_c = 0.03 – 0.05 and v_d = 0.05 – 0.1 cm/s.

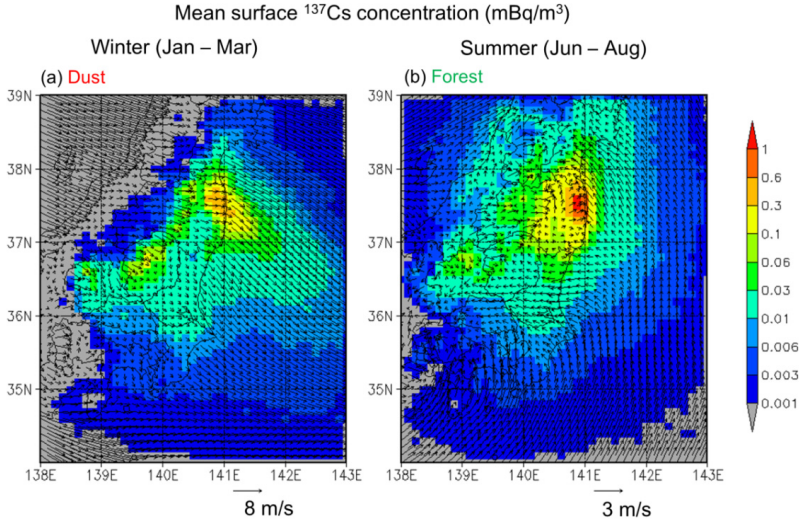

Figure 10. Seasonal mean surface (10 m above ground level) wind vector and ^{137}Cs surface concentration (a) due to dust re-suspension in winter from January to March and (b) due to forest re-suspension in summer from June to August. The deposition parameters of the simulation in the figure are E_c = 0.04 and v_d = 0.1 cm/s.

Atmos. Chem. Phys. Discuss., doi:10.5194/acp-2016-270, 2016
Manuscript under review for journal Atmos. Chem. Phys.
Published: 25 April 2016

Atmospheric Chemistry and Physics Discussions

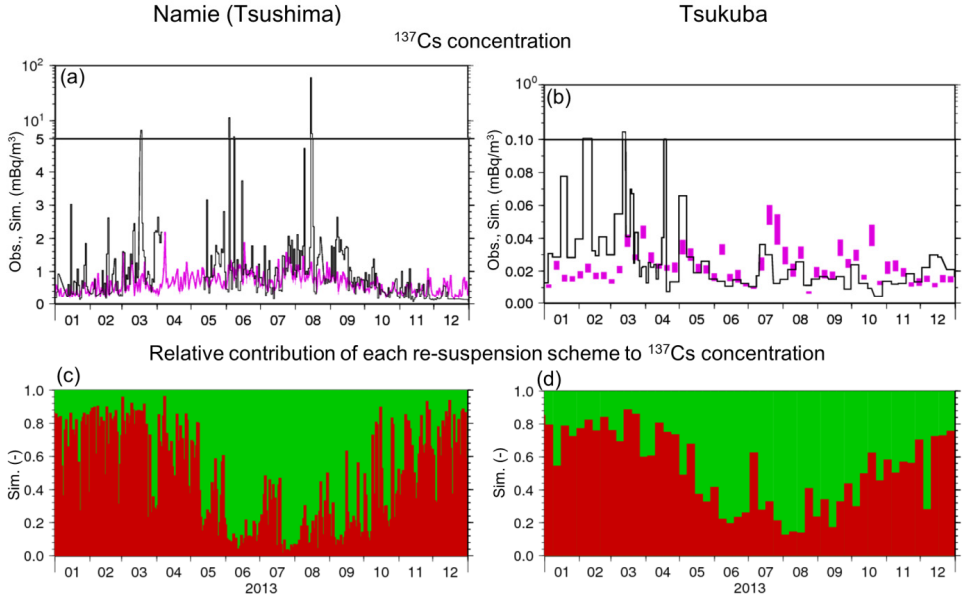

Figure 11. Time series of (a, b) (black) the observed and (purple) the simulated surface ^{137}Cs concentration due to total re-suspension and (c, d) the relative contribution of (red) dust and (green) forest re-suspension to the ^{137}Cs concentration at (a, c) Namie and (b,d) Tsukuba. The shaded areas of (1) and (b) indicate the range of ^{137}Cs concentrations obtained when the simulations were run using the optimized parameter ranges E_c = 0.03 – 0.05 and v_d = 0.05 – 0.1 cm/s.

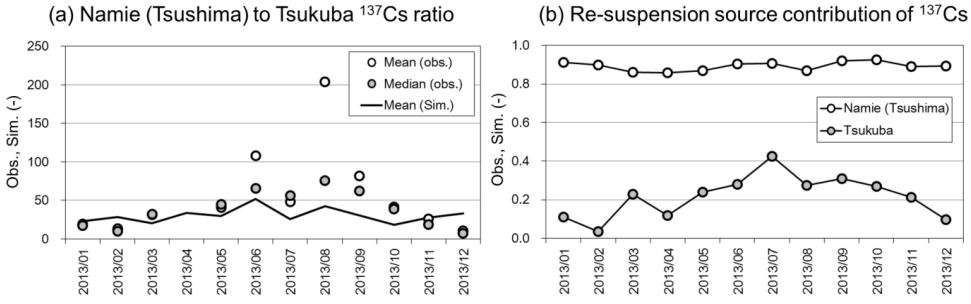

Figure 12. Monthly mean (a) observed mean, observed median and simulated Namie to Tsukuba ^{137}Cs concentration ratio and (b) simulated re-suspension source area (where the observed deposition amount > 300 kBq/m^2) contributions to ^{137}Cs air concentration at Namie and Tsukuba. The deposition parameters of the simulation in the figure are E_c = 0.04 and v_d = 0.1 cm/s.

Atmos. Chem. Phys. Discuss., doi:10.5194/acp-2016-270, 2016
Manuscript under review for journal Atmos. Chem. Phys.
Published: 25 April 2016

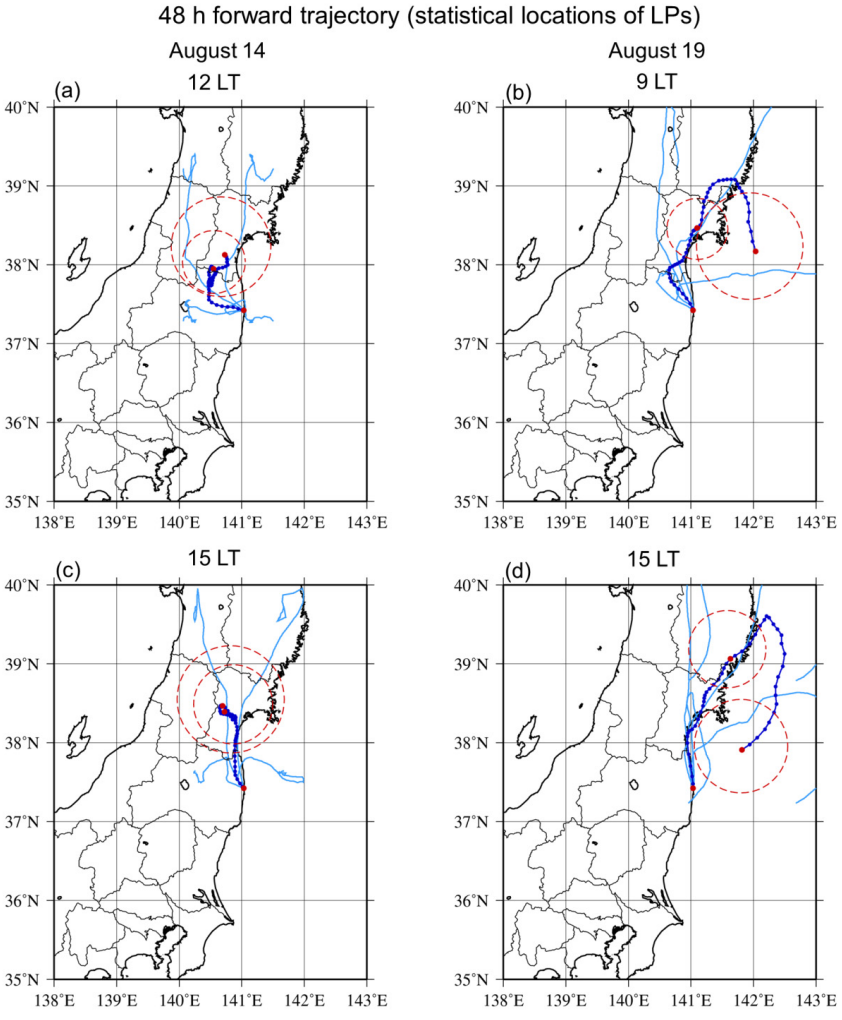

Figure 13. 48 h forward trajectory (statistical locations of LPs within 1 km AGL) predicted by the LM starting at (a) 12 LT and (c) 15 LT of August 14 and (b) 9 LT and (d) 15 LT of August 19. Blue lines indicate median locations of LPs at 1 h and 1 d intervals as blue and red dots, respectively. Sky-blue lines indicate 17th and 83rd percentile locations of LPs and red dashed circles indicate areas containing 66% of the LPs.

Atmos. Chem. Phys. Discuss., doi:10.5194/acp-2016-270, 2016
Manuscript under review for journal Atmos. Chem. Phys.
Published: 25 April 2016

Atmospheric Chemistry and Physics Discussions

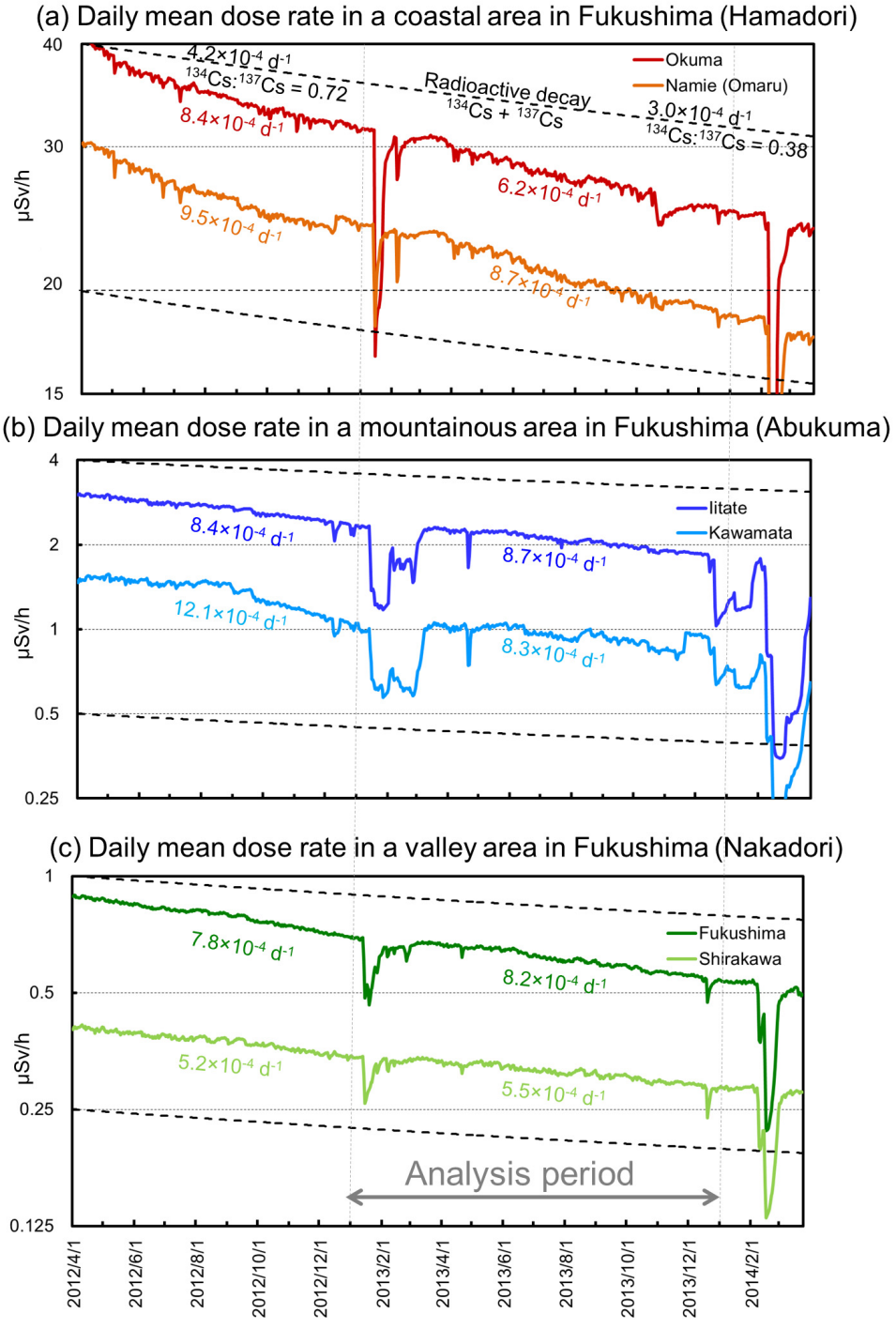

1

Atmos. Chem. Phys. Discuss., doi:10.5194/acp-2016-270, 2016
Manuscript under review for journal Atmos. Chem. Phys.
Published: 25 April 2016

Atmospheric Chemistry and Physics Discussions

Figure C1. Daily mean gamma dose rate at the six monitoring sites: (a) (red) Okuma town and (orange) Namie town (Omaru district) in the coastal area, (b) (blue) Iitate village and (sky blue) Kawamata town in the Abukuma highland area, and (c) (green) Fukushima city and (greenish yellow) Shirakawa city in the Nakadori valley area of Fukushima prefecture as presented in Fig. 1b for two fiscal years (from April 2012 to March 2014). The first-order decreasing rates of the least-square approximation over the period of no snow cover (May to October, 2012 and 2013) is also presented, along with the radioactive decay (^{134}Cs plus ^{137}Cs, by assuming the same amount of activity on March 12, 2011) in April 2012 and March 2013.